

THE GEOMETRY AND MICROSTRUCTURE OF A RANGE
OF QP-MYLONITE ZONES - A FIELD TEST OF THE
RECRYSTALLIZED GRAINSIZE PALAEOPIEZOMETER.

M.A. Etheridge and J.C. Wilkie

Dept. of Earth Sciences,
Monash University,
Clayton, Victoria, 3168,
AUSTRALIA.

INTRODUCTION

Sibson (1977) has proposed a "two-layer" model for large fault zones in which an upper elasto-frictional (EF) regime passes downward into a quasi-plastic (QP) regime where dislocation flow processes dominate. In this model he suggests that the resistance to shear in the zone is a maximum in the region of the transition between the two regimes (Sibson, 1977, fig.8). Depending on the rate of decrease of shear resistance with depth in the QP regime, it is thus predicted that the shear stress in much of the seismic section of the fault zone will be similar to that in the QP regime, especially the upper parts. In this context, any means of determining palaeostress magnitudes from the structures in QP mylonites is important to an understanding of the stresses responsible for seismic failure.

Recent experimental (Goetze, 1975; Raleigh and Kirby, 1970; Kohlstedt et al, 1976; Mercier et al, 1977; Ross et al, 1977) and theoretical (Miss, 1977) studies have underlined the potential of a variety of microstructural parameters as indicators of shear stress magnitudes during steady state dislocation flow of a number of minerals. Dislocation flow is the dominant deformation mechanism in QP mylonites (Bell and Etheridge, 1973). The most easily measured of these microstructural parameters is the dynamically recrystallized grain size, and the widespread occurrence of dynamic recrystallization in the QP regime (it is the dominant means of grain size refinement in mylonites, White, 1973, 1977; Bell and Etheridge, 1973) gives it broad applicability to this problem.

This paper describes the results of a study of the microstructure, recrystallized grain size and, to a lesser extent, larger scale structures of a variety of QP mylonite zones transecting quartz bearing rocks. The primary aim of the study was to assess the applicability of the published relationships between stress and recrystallized grain size to naturally deformed mylonites, but in all cases the structure of the zones on all scales was either well established or recorded during the study. The mylonite zones examined fall into three distinct tectonic categories.

1) Thrusts and thrust nappes of the northern margin of the intracratonic Amadeus Basin (Forman, 1971; Forman and Shaw, 1973). These structures occur in local areas of intense deformation, and are developed in pure quartzites. They are largely supracrustal structures presumably related to movement on deep-seated basement faults.

2) The Woodroffe and Davenport thrusts in the Musgrave Ranges, central Australia occur within high grade gneisses and granulites, and must have originated deep in the crust (Major et al, 1967; Bell and Etheridge, 1973, 1976; Bell, 1978).

3) Near vertical faults with significant horizontal components of movement are widespread throughout the Palaeozoic granites of the Lachlan fold belt in south-eastern Australia. Displacement of topographic features shows that movement on some of these faults has been quite recent, and they may be responsible for the low level seismicity of the area (Cleary et al, 1964).

The location of each of these three groups of fault zones is shown in figure 1. Their geological setting, microstructural development and recrystallized grain size will be described in turn, followed by a discussion

of the stress/grainsize relationships and their relevance to QP mylonites. The methodology of grainsize measurement and the criteria used to select suitable samples for measurement are discussed in Appendix 1.

THRUSTS AND THRUST NAPPES OF THE NORTHERN AMADEUS BASIN

General Geology

The Amadeus Basin, a large intracratonic depression, is filled with marine sediments ranging in age from upper Proterozoic to Carboniferous. The northern boundary of this basin outcrops just south of Alice Springs (figure 2) and runs east-west for several hundred kilometers. Underlying the Amadeus Basin sediments are the older Precambrian metamorphic rocks that comprise the Arunta Complex.

The Arunta Complex consists of multiply deformed gneisses, schists and quartzites which range in metamorphic grade from lower amphibolite to granulite facies (Marjoribanks, 1974, 1976; Wilson, 1970). The last major deformational event, the Alice Springs orogeny (358-322 Ma., Stewart 1971) also involved the overlying Amadeus Basin sequence. Deformation of this age is localized, and apparently resulted from reactivation of large basement faults (Forman, 1971; Fonnán and Shaw, 1973; Marjoribanks, 1974). Both Amadeus Basin sedimentary rocks and basement gneisses were thrust southwards in a series of large fold and thrust nappes (Forman, 1971). Thrust zones on scales from a few mm to tens of metres are best developed in the basal unit of the cover sequence, the Heavitree Quartzite. This unit consists dominantly of relatively pure orthoquartzite, with minor interbedded conglomerate and siltstone, and is Upper Proterozoic in age.

The most extensive development of thrusting in the Heavitree Quartzite is found northeast of Alice Springs in the Arltunga nappe complex. In the Atnarpa area of this complex (figure 3), a number of superimposed shallow dipping thrust sheets have been mapped in detail by Yar Khan (1972). Detailed structural analysis and microfabric studies showed that there was a gradual change from ductile deformation in the north of the area to brittle deformation in the south and west during thrusting. Yar Khan (1972) suggested that this is consistent with lower level, and thus higher temperature rocks being thrust up from the north and east. In order to investigate the effect this has had on recrystallized grainsize, several suites of quartzites were collected across thrusts throughout this area. The locations of the traverses are given in figure 3.

A similar, although less extensive, series of thrusts is exposed in the Ormiston area, 200 kms west of Alice Springs. Heavitree Quartzite, from two of these thrusts, has been sampled in a similar manner to the Arltunga nappe complex and figures 4 and 5 respectively show the sample localities and the detailed geology of the Damper Gorge section.

North of the Amadeus Basin sediments large, more steeply dipping faults are exposed in the basement rocks. These are the deeper equivalent of the more shallow dipping thrusts seen in the overlying sediments (Marjoribanks, 1974). In all cases there is ductile deformation of the rocks adjacent to and within these fault zones. Of particular interest is a large mylonite zone in the Chewings Range Quartzite at Fish Hole (figure 2).

This structure marks the southern boundary of this quartzite range and a number of samples have been collected across the mylonite zone.

Detailed Geology, Microstructure and Grainsize

Arltunga Nappe Complex - Six separate exposures were sampled in the Arltunga nappe complex (A to F in fig.3), comprising the range of ductile to brittle microstructures. At locality A, mylonitized Heavitree Quartzite between two parallel thrusts is uniformly fine grained (table 1) and totally recrystallized (fig. 7a), with a strong mylonitic schistosity. At Ruby Gorge (loc. B), a continuous section is exposed, from undeformed quartzite with gradually increasing strain to totally recrystallized mylonite. The finite strain within the quartzite can be determined at low to moderate strains from the shapes of the initially equant and well rounded detrital quartz grains (Marjoribanks, 1976). As the original grains become more elongate, the proportion of recrystallized quartz increases (fig.7 b-d), until recrystallization is complete and a steady state, fine grained microstructure persists right up to the thrust contact with the basement gneisses. The recrystallized grainsize is remarkably constant with increasing strain, except that there is a significant increase that coincides with complete recrystallization (fig.6, fig.7 b,e). A very similar traverse with a finite strain gradation up to a thrust contact was sampled at locality C, and the microstructures and grainsize are very similar to Ruby Gorge. The Heavitree Quartzite at locality D outcrops as a number of thin (1 to 5 m) layers and lenses within mylonitized basements. All samples from these tectonically emplaced "slices" are totally recrystallized, and the grainsize is quite uniform despite the variation in finite strain that must exist within and between slices (fig.6).

In the south of the area (loc. E and F), the fault zones are typically occupied by dark coloured quartzites with a brecciated appearance. The microstructures of these rocks are complex, but indicate that a period of plastic deformation was overprinted by a more brittle event. Figure 8 (a-c) illustrates the variation in microstructure with increasing plastic strain from locality E; the relict grains have a more cold-worked appearance and the recrystallized grainsize is uniformly fine (fig.6). Several generations of discrete shear zones, fractures and quartzfhematite veins overprint this microstructure. These structures suggest more brittle behaviour, although fibrous vein filling and strain shadowed grains within shear zones (fig.8 d, e) indicate that failure was not totally catastrophic. The grainsize within the shear zones is the same as that in the remainder of the rock, and insertion of a λ -plate shows that both have a similar, strong crystallographic preferred orientation, consistent with the operation of dynamic recrystallization throughout. At the southernmost locality, F, the detrital quartz grains are only slightly elongate and are commonly angular, even close to the thrust contact. Optical evidence of dynamic recovery and recrystallization is very limited, and discrete fractures and veins are common (fig.8f). It is considered that these southern thrust zones were deforming very close to the brittle-ductile transition, with an increasing tendency for brittle behaviour as thrusting progressed.

Ormiston Area - Damper Gorge cuts through the quartzite range at right angles to strike, exposing two large thrust zones dipping at 40° towards the north (fig.5). Figure 9(a-c) shows the range of microstructure with increasing strain in both of these thrust zones. There is no significant difference between them, but they differ from the Ruby Gap sequence in the following ways:-

(i) Deformed original grains tend to be strain shadowed or deformation banded rather than polygonized into subgrains.

(ii) Finite strain recorded by original grain shape is higher for a given proportion of recrystallization.

(iii) Recrystallized grain size is finer (15 to 25 μm), and does not increase in completely recrystallized samples (fig.6).

Ormiston Gorge exposes a shallow dipping thrust plane that truncates the lower limb of a large mesoscopic fold. Again, we have collected a suite of samples from almost undeformed quartzite with increasing strain into the thrust zone. However, in this case, recrystallization is much more limited, finer grained (fig.6) and even the most highly deformed samples contain original grain remnants (fig. 9 d-f). In general, the microstructural trends noted above are even more evident.

Thrusts Within Arunta Complex Basement - In the Chewings Range (fig.2), quartzites, schists and felsic gneisses are all transected by a number of macroscopic fault zones. It is of particular interest to compare the response of the basement Chewings Range quartzite to mylonitization with that of the Heavitree Quartzite from the cover sequence. The locality selected is at Fish Hole, where Jay Creek cuts through the southern part of the Chewings Range.

Here, a mylonite zone approximately 10 m wide and dipping 80° towards the south, thrusts gneisses over the quartzite (fig.8). The Chewings Range Quartzite outside the fault zone is a very coarse-grained metamorphic quartzite with 2 to 5% sillimanite as the only significant impurity. The quartz grains are roughly equidimensional, and have the complex grain boundary shapes typical of materials at advanced stages of exaggerated grain growth (Wilson, 1973). The change in microstructure with increasing strain is seen in figure 10 (a-c). These microstructures are an extension of the trend already noted for the Ruby Gap \rightarrow Damper Gorge \rightarrow Ormiston Gorge suites. Original grains are highly flattened without substantial recrystallization, and sharply bounded, high angle deformation bands are common. Recrystallization is confined to grain and deformation band boundaries even at quite high strains (fig.10d), although it extends to grain interiors where subgrains are best developed (fig.10c). Once again recrystallized grain size is independent of strain within the mylonite zone, in this case between 7 and 11 μm throughout (fig.6).

WOODROFFE AND DAVENPORT THRUSTS

General Geology

The Musgrave Ranges in north-western South Australia consist largely of high grade felsic gneisses and granulites. The ranges run east-west, parallel to a number of major reverse faults. The best exposed of these structures is the Woodroffe thrust, which can be traced for over 300 km, and which separates granulite facies rocks in the south from amphibolite facies gneisses to the north. The fault zone, which is up to 1 km wide in outcrop, dips at about 30° south, and the granulites comprise the overthrust block. 10 to 30 km to the south, a parallel structure, the Davenport thrust has overthrust a series of amphibolite to transitional granulite facies gneisses

onto the granulites (fig. 11). The metamorphic and structural geology of the Amata area has been described by Collerson et al (1972), and figure 12 is modified from their paper. The traverse across the Woodroffe thrust in the north of the area was sampled as part of a detailed study of the mylonites (Bell and Etheridge, 1973, 1976; Bell, 1978), and in the south we have selected samples from Collerson's collection, mainly to study the effects of the Davenport thrust. In both cases, mylonitization has been restricted to a narrow (a few tens of meters) zone within the granulites, but has been much more widespread (up to several km from the main zone) in the lower grade gneisses.

Microstructures and Grainsize

The microstructures of the Woodroffe thrust mylonites have been described in detail by Bell and Etheridge (1973, 1976). They showed that the overthrust granulite facies gneisses have reacted quite differently to the underlying amphibolite facies rocks during mylonitization (compare figures 9 and 12 from Bell and Etheridge, 1976). We have remeasured the recrystallized grainsizes so as to maintain internal consistency, and figure 13 plots grainsize against position within the thrust zone (quartz-solid line, feldspar-dotted line), together with a qualitative estimate of finite strain magnitude (dashed line - see fig. 13, Bell and Etheridge, 1976). The quartz grainsize is relatively uniform within the mylonitized amphibolite facies gneiss, and is about four times that found on the granulite facies side. This difference in grainsize parallels a marked difference in a range of other microstructural parameters. In particular, dynamic recovery and recrystallization take place at much lower finite strains in the lower grade gneisses.

Bell and Etheridge (1976) have attributed most of these differences to hydrolytic weakening effects in the "wetter" amphibolite facies gneisses. The total H₂O content of the granulites and gneisses is 0.2% and 1.0% respectively. Considering the assemblages in each, it is thus likely that the activity of H₂O in the amphibolites was significantly higher than in the granulites during mylonitization. This is expected to have had a marked effect on the solubility of hydrous species in quartz and other structurally anhydrous phases. They considered that the stress was unlikely to have varied significantly across the mylonite zone during ductile flow, and explained most of the microstructural differences (including recrystallized grainsize) in terms of a climb-related hydrolytic weakening model. We shall consider the ramifications of this in a later section.

The Davenport thrust zone south of Amata provides an excellent opportunity to test the extent of this hydrolytic control on recrystallized grainsize. Here, the gneisses of "transitional terrain" of Collerson et al (1972) are thrust over the same body of granulites involved in the Woodroffe thrust (fig. 12), and they have a range of total H₂O contents intermediate between the amphibolite facies gneisses and the granulites. Simplistically, we might thus expect them to have intermediate recrystallized grainsizes. Because we could not gain access to this area, we have had to rely on Collerson's sampling, which was not primarily designed to study the mylonites. The location of samples is shown in figure 12 and the grainsize data are summarized in table 1.

There appears to be a patchy development of assemblages representing a range of metamorphic conditions within the transitional terrain. Partly mylonitized rocks are found up to 5 km from the main thrust zone within the transitional block, but there are only a few metres to a few tens of metres of mylonitized granulites in the footwall. Comparison of the grainsize data with sample location shows that grainsize does not depend strongly on distance from the thrust, but examination of the pre-mylonitic assemblages reveals a good correlation between grainsize and the proportion of hydrous minerals (table 1). The few specimens apparently collected from the granulite side of the thrust have recrystallized grainsizes less than 30 μm , whereas those from the transitional terrain range from 30 to 100 μm . This range of grainsizes bridges the gap between the mean values from the two sides of the Woodroffe thrust, and provides very good support for a hydrolytic control.

Felspar (both perthite and plagioclase) has recrystallized in many of these samples, and its grainsize is also given in table 3. Feldspar grainsize is $\frac{1}{5}$ to that of quartz in the same specimen, but there is a good correlation between them.

STEEPLY DIPPING FAULTS IN GRANITES OF THE LACHLAN FOLD BELT

The Lachlan fold belt is the southernmost tectonic entity within the lower Palaeozoic to Mesozoic Tasman fold belt that occupies much of eastern Australia. Its geology and tectonic development have recently been discussed by Packham (1969); Scheibner (1974 a,b); Solomon and Griffiths (1972); Douglas and Ferguson (1976) and Rutland (1976). Granitic (sensu lato) bodies are widespread throughout the fold belt (fig.14) ranging in age from Ordovician to Carboniferous (Evernden and Richards, 1962; Brooks and Leggo, 1972; Chappell and White, 1974; White et al, 1974) and commonly contain deformed zones in which mylonitic rocks are developed. These deformed zones range from narrow (<1 m) bands of mylonite, through larger but discrete mylonite zones that correspond to mappable faults, to broad (>1 km), sub-planar regions of foliated granite that generally contain one or more discrete highly deformed zones.

Foliated Granites and Their Associated Mylonites

General Geology

Tectonically foliated granites are widespread in the Lachlan fold belt, and they extend over the range of geochemical affinities (S- and I-types, Chappell and White, 1974). The foliation and lineation are generally concordant with the dominant structures in the folded country rocks, and are considered to result from the same deformation event (Hobbs, 1965; White et al, 1977). We have selected the Wondalga (fig.15) and Wyangala (fig.16) granites for this study. Both intrusives are generally at least weakly foliated, and they contain broad meridional zones in which the foliation is more intense and discrete mylonite zones are developed. In each sample location, we have tried to include a range of foliation development (i.e., finite strain).

Microstructures and Grainsize

The typical mineralogy of these granites is quartz + plagioclase + biotite \pm IC-feldspar \pm hornblende \pm muscovite. The microstructural res-

ponse to deformation is largely controlled by the behaviour of the quartz and feldspar, although the mica plays an increasing role as mylonitization becomes more advanced. In all of the rocks examined, quartz has been ductile and has recrystallized readily, even at low strains, whereas feldspar may have been rigid, ductile or essentially brittle in its response. In all cases, feldspar was significantly stronger than quartz. Biotite deforms readily but is slower to recrystallize than quartz, although it tends to disperse throughout the rock at higher strains. In general, the deformational microstructures of these rocks are very similar to those from other mylonitized rocks of the same broad mineralogy (Hobbs, 1966; Bell and Etheridge, 1973, 1976). They are well suited to this study, because the quartz recrystallizes readily, and recrystallized aggregates derived from a single original grain remain coherent and monomineralic to quite high strains. Figure 17 shows the typical changes in microstructure with increasing strain from weakly foliated granite to mylonite.

Recrystallized quartz grainsizes within this group tend to be coarser than the central Australian examples (table 2). There is some variation between the more widely spaced groups of sample locations, but the values are once again very consistent from sample to sample at any one location. This is especially true in the Wyangala granite, where three widely separated localities have significantly different mean grainsizes, but there is very little internal variation. In particular, the grainsize is largely independent of strain, although the Wondalga granite samples show some tendency for finer grainsizes in the weakly deformed and recrystallized samples.

Fault-like Mylonite Zones in Granite

We have studied several major (10-500 km) fault zones which contain mylonitized granite, and two of them are of particular interest. The first is found along the eastern margin of a major ophiolite (Coolac serpentine belt) and may represent a fossil obduction zone, while the second (Crackenback fault) shows evidence of Recent movement and possibly present day seismic activity.

Coolac Serpentine Belt

General Geology - The Coolac serpentine belt is a classical narrow, fault-bounded Alpine-type ultramafic belt. It can be traced for about 500 km, but is best exposed at its southern end, between Coolac and Goobarragandra (Golding, 1969; Ashley *et al*, 1971; Ashley and Chenhall, 1976), (fig. 15). Along the whole of this section, the ultramafics are bounded on their eastern side by foliated to mylonitized felsic intrusives of the Young Granodiorite (410-420 Ma, Ashley *et al*, 1971). The deformation of the granodiorite has been ascribed to the emplacement of the ultramafic rocks, and can be confidently dated between 400 and 385 Ma (Ashley *et al*, 1971). Ashley and Chenhall (1976) have interpreted the belt as an ophiolite, and its emplacement to obduction during the middle Devonian regional folding event.

Microstructure and Grainsize - The general microstructure of the mylonites have been described by Ashley and Chenhall (1976) and we have collected specimens from a selection of their localities (fig. 15). The microstructures are, in fact, more complex than they recognised, and the quartz shows the effects of two discrete deformation events. Isolated quartz aggregates generally consist of elongate and variably deformed grains which have themselves undergone some recrystallization (fig. 18, and also fig. 6 of Ashley and Chenhall, 1976). It is apparent that the quartz has

been coarsely recrystallized during an earlier event, and that these recrystallized grains have been deformed during the main mylonitization. Very little recrystallization accompanied the second deformation, which is characterized by ribbon-like grains with strong undulose extinction, sharp deformation bands, serrated grain boundaries and little subgraining on the optical scale. Ashley and Chenhall (1976) describe the Young Granodiorite as massive to weakly foliated throughout much of its outcrop area, with the foliation stronger as the contact with the ultramafics is approached. Because of the over-printing deformation, it is difficult to measure the grain size of the earlier generation of recrystallized grains, but they are in the range 80 to 100 μm . These values correspond well with those from the foliated granites in the previous section, and we believe that they have the same origin, that is, they reflect weak to moderate straining of the granodiorite during a regional deformation event prior to the emplacement of the ultramafic belt. The paucity of recrystallization attributable to this later deformation makes the grain size difficult to measure accurately, but it is very fine, generally in the range 6 to 12 μm , and does not vary greatly with finite strain.

Crackenback Fault

General Geology - The Crackenback fault is traceable for 45 km within the felsic intrusives of the Kosciusko Batholith and the surrounding Ordovician slates and greywackes (White et al, 1977). It trends towards 050°, and its straight outcrop trace in rugged terrain suggests that it is steeply dipping (fig. 19). In the Thredbo area, the fault traverses the Mowambah Granodiorite (White et al, 1977), and occupies the valley of the Crackenback River, which separates two distinct topographic levels. The average height of the dissected Miocene peneplain is 300 to 400 m higher on the northwestern side, suggesting that the Crackenback fault is a locus of the Pleistocene to Recent uplift in this area. This is supported by the tentative epicentre location for an earthquake in this region in 1959 (Cleary et al, 1964).

The Mowambah Granodiorite is generally well foliated, even several kilometres from the fault, and narrow (1 - 10 m) mylonite zones occur throughout the area of figure 19, although they are more closely spaced within one kilometer of the Crackenback River. Most importantly, however, neither the regional foliation nor the mylonitic foliation (they sometimes crosscut) are parallel to the topographic expression of the fault. Unfortunately, outcrop is very scarce in the river valley itself, but isolated outcrops of mylonite were found in which the foliation is parallel to the fault. This area is of particular interest because it contains all of the following:-

(i) Foliated granite of the same type as that described in the previous section.

(ii) Discrete mylonite zones, some of which overprint the regional foliation.

(iii) Evidence of recent fault movement; in fact, it may tentatively be classed as an active fault.

(iv) A small stock of massive granodiorite that intrudes the foliated granodiorite and is cut by the fault.

Microstructure and Grainsize - The Mowambah Granodiorite is at least weakly foliated over most of its outcrop area (White et al., 1977). It is a coarse grained "S-type" granite (Chappell and White, 1974) containing quartz + plagioclase + K-feldspar + biotite + minor muscovite. The foliation is defined by flattened quartz grains and more or less well oriented biotite. Feldspar is only plastically deformed at high bulk strains. In most specimens, there is evidence of two episodes of deformation. The first, which is associated with the regional foliation and the bulk of the mylonitization, has been responsible for a gross microstructure very similar to that described above for the Wyangala granite (fig. 18). In particular, it was accompanied by extensive, relatively coarse recrystallization of quartz (80 to 150 μm , table 5). There is some evidence that the narrow mylonite zones which overprint the regional foliation have grain-sizes in the lower end of this range, but this has not been clearly established from the samples available. These coarsely recrystallized grains are quite strongly undulose, invariably have serrated grain boundaries, and are commonly elongate at an angle to the main foliation (fig. 18). Recrystallization is not commonly associated with this later deformation, but where it is grain-sizes range from 15 to 30 μm (table 3).

The small granodiorite stock at the north-eastern end of the Crackenback River valley (fig. 19) has an I-type mineralogy (quartz + plagioclase + hornblende + biotite + K-feldspar), and is only very weakly deformed. None of the phases has undergone more than isolated recrystallization and most quartz grains contain a coarse (50 - 100 μm) blocky subgrain structure, deformation lamellae and a number of subparallel fractures or narrow shear zones (fig. 20).

Some of the shear zones within the quartz grains contain both brittle and ductile deformation structures, and traverse a number of grains. They consist of an array of roughly orthogonal fractures in a zone about 200 μm wide, associated with local undulose extinction (fig. 20). A zone may be located within a single deformation band, or it may cut across the coarse substructure. There is a very strong preferred orientation of the trace of these zones in thin section and a weaker but significant alignment of the larger discrete fractures within quartz grains.

DISCUSSION

The main emphasis of the discussion will be on recrystallized grainsize and its usefulness as a palaeopiezometer. In all of the QP mylonite zones studied, quartz has deformed by the same range of dislocation flow, dynamic recovery and dynamic recrystallization mechanisms that have been widely reported elsewhere (White, 1973, 1977; Bell and Etheridge, 1973, 1976). It is thus apparent that flow models based on these mechanisms are suitable for QP regime mylonites in which quartz controls the mechanical response. The role of feldspar and mica in deformed felsic gneisses and intrusives is much more complex, however, and understanding of the mechanical response of these phases is very important. For example, feldspar deformation mechanisms ranged from purely brittle (\pm twinning) in some of the granites in fault zones to largely ductile (dominated by dislocation creep and recrystallization) in the Woodroffe and Davenport thrusts. Mica becomes most important at advanced stages of mylonitization, where it begins to be dispersed throughout the recrystallized quartz and/or feldspar aggregates to form a slaty or phyllitic rock that is mineralogically homo-

geneous on the scale of the fine mylonitic grainsize. This grainsize is largely controlled by interfacial energies between phases and diffusion rates of the major components, and it is not useful as an indicator of stress. Deformation of these slaty mylonites is controlled largely by diffusional and grain boundary processes rather than dislocation flow.

Conclusions From Recrystallized Grainsize Data

A number of important and consistent relationships between recrystallized grainsize, microstructure and larger scale structure have been found. These relationships have important implications for discussion of stress/grainsize equations and their applicability, and so we summarise them here as a prelude to that discussion.

(i) Recrystallized quartz and feldspar grainsize is largely independent of finite strain within a single mylonite zone. This is true across the whole range of grainsizes and tectonic settings encountered in this study. The major exception to this rule is the jump in grainsize that accompanies total recrystallization in mylonitized Heavitree quartzite.

(ii) In a given mylonite zone, recrystallized grainsize varies with parent rock composition and/or mineralogy. We have strong evidence that bulk H₂O content is the major control, and that this is related to hydroxyl species in the quartz and feldspar structures which affect deformation and/or recovery processes (cf. hydrolytic weakening). The best evidence comes from the Woodroffe and Davenport thrusts, where the granulite facies ("dry") rocks occur in the hangingwall and footwall respectively, and recrystallize to identical grainsizes. However, gneisses containing more hydrous assemblages give rise to coarser grainsizes, again independent of position with respect to either thrust.

(iii) Systematic variations in grainsize with tectonic setting are not as clear, but the higher temperature zones (Musgrave Range and regionally foliated granites) presumably represent deeper structural levels, and are all consistently coarser grained. The Crackenback fault shows evidence of a coarse recrystallized grainsize associated with a regional foliation overprinted successively by individual mylonite zones of intermediate grainsize, a fine grainsize associated spatially with the major fault and a final brittle event.

(iv) There is a strong and consistent relationship between recrystallized grainsize, the range of optical deformation microstructures, and the rate of recrystallization with respect to finite mylonitic strain. Specifically, the coarser grained mylonites recrystallize at lower strain and are accompanied by extensive optical evidence of "easy" recovery. In contrast, rocks with finer recrystallized grainsize have a more "cold worked" optical microstructure, and original grains are highly strained before they substantially recrystallize.

(v) Recrystallized feldspar grainsize is generally one-third to one-fifth that of quartz in the same rock, and there is a fair to good correlation between quartz and feldspar grainsize at any locality. This correlation is particularly good in the Woodroffe and Davenport thrusts, suggesting that a hydrolytic control on grainsize also operates in feldspar. We have found no significant difference between plagioclase and alkali feldspar.

In summary, our data strongly support the concept of a steady state dynamically recrystallized grainsize that is largely independent of finite strain. However, this grainsize is apparently critically dependent on the ease of dynamic recovery, and variables that affect this (e.g., temperature "H₂O" content) have a direct bearing on the grainsize.

Discussion of Stress/Grainsize Equations

It has been recognised for some time that materials undergoing steady state dislocation creep develop a stable microstructure, and that several parameters of that microstructure are related uniquely to the deforming stress (Bird et al, 1969). The most useful of these parameters are dislocation density, subgrain size and recrystallized grainsize. Recently a theoretical relationship between creep stress, subgrain size and recrystallized grainsize has been developed that can be readily applied to minerals (Twiss, 1977).

Twiss' model is attractive because it gives a simple relationship of the expected form, is apparently independent of mechanism, and fits very well with the experimental data for metals and alloys. The limited experimental data for minerals are of questionable quality because the stress measurements were made in a solid pressure medium deformation apparatus, but they compare well with Twiss' theory, and an empirical stress/grainsize formula for quartz (Mercier et al, 1977) is discussed below. Before applying Twiss' theoretical stress/grainsize relationship to the data from the previous chapter, the derivation of the formula and the assumptions inherent in applying it will be discussed.

The basic assumptions involved in deriving the stress/grainsize relationship are (Twiss, 1977 and unpubl. mss.):-

(i) Subgrains and recrystallized grains are of minimum possible size, with the proviso that the total strain energy of the dislocations in a closed boundary of a subgrain or recrystallized grain is equal to the total strain energy of the dislocations distributed within the bounded volume.

(ii) The Taylor back-stress relationship between differential stress (σ) and steady-state dislocation density (ρ) is accepted. These assumptions lead to a relationship between differential stress (σ) and either subgrain or recrystallized grainsize (d) of the form,

$$\Gamma \sigma = K \left(\frac{d}{b} \right)^{-p} \quad (1)$$

where $\Gamma = \mu/(1-\nu)$, μ is shear modulus, ν is Poisson's ratio, b is Burgers vector of dislocations, and K and p are material constants that depend upon dislocation and boundary energy terms. Unique determination of K and p is difficult, but Twiss showed that empirical values obtained from published data fit well within the rather narrow expected ranges for these parameters. Twiss' final equations are thus:-

$$\text{for subgrains: } \sigma = 8.1 \Gamma \left(\frac{d}{b} \right)^{-1} \quad (2)$$

$$\text{for recrystallized grains; } \sigma = 2.4 \Gamma \left(\frac{d}{b} \right)^{-0.68} \quad (3)$$

It should be noted that these equations are independent of strain and temperature, which is consistent with the metallurgical data.

There are a number of possible criticisms of Twiss' derivation of these equations. First, there is some question of the relevance of the Taylor back-stress model to the dynamic situation (Twiss, pers. comm.), even though it agrees well with the reliable experimental data from metals and alloys (Bird et al, 1969). A more serious criticism can be levelled at the derivation of the boundary and volume energy terms in the recrystallized grainsize analysis. The dislocation loop expansion model for formation of a recrystallized grain seems somewhat simple-minded, and this could particularly affect the value of p in equations 3 and 5. However, there seems to be a real inconsistency in applying the first assumption above to a recrystallized grain which is free of dislocations, since the volume energy term must then be zero. Even though Twiss' model produces a dislocation-free recrystallized grain, the energy balance calculation assumes an internal dislocation density given by the Taylor back stress model. The high degree of fit between the model and the metallurgical data, however, suggests that these problems are not critical to its application, and that the form of equation 1 is reasonable. The values of the constants K and p , however, provide a possible source of significant error.

The experimental data used to determine the values of K and p in equations 2 and 3 are primarily derived from metals and alloys. Although the few data for quartz are also used in the regression, they are the furthest from the mean line (Twiss, 1977, fig. 1), and significant variation in the value of K seems possible between different materials. The main influence on the value of K comes from the dislocation interaction term α . The value for metals is well constrained at about 0.7 (Bird et al, 1969), but the only experimentally determined value for a mineral (olivine) is 2.3 (Kohlstedt et al, 1976) and the value determined by Twiss (1977) from his regression of all data is 1.57. The constant K varies from 1.1 to 3.5 for the α range from 0.7 to 2.3, which gives approximately 6 times difference in grainsize for the same stress. In terms of the grainsize data presented earlier, this is a most significant variation, and careful determination of α for quartz and feldspar is most important for application of the Twiss relationship.

In contrast, the value for p seems much better constrained, and even a large variation from 0.6 to 0.8 produces only about a twofold increase in grainsize for stresses in the expected range.

The important features of the recrystallized grainsize data collected in this study have been summarized above. The independence of recrystallized grainsize and finite strain is clearly consistent with the Twiss model, but the effect of H_2O through a "hydrolytic weakening" process or a temperature dependence of grainsize are not. At first sight, it is difficult to see why either water content or temperature should affect the steady state grainsize at a particular stress. Certainly as both increase, the rate of recovery increases (Hobbs et al, 1972), and the strainrate rises at constant stress. However, the balance between strainrate and recovery rate should give rise to a constant dislocation density, and thus a constant recrystallized grainsize according to Twiss' model. Neverthe-

less, there is no doubt from the data that water, in particular, substantially affects grain size, and we believe that this can only be satisfactorily explained by a stress/grain size model that is directly related to the operative recovery/recrystallization mechanisms.

The optical microstructures in almost all of the rocks examined during this project indicate that recrystallization takes place by a mechanism of the subgrain rotation type (Hobbs, 1968; Bell and Etheridge, 1976; Poirer and Nicolas, 1975). This mechanism involves the progressive increase in misorientation between adjacent subgrains during the dynamic recovery/recrystallization process. In support of such a model, transitions are commonly found from weakly undulose subgrained recrystallized within a variably strained quartz or feldspar grain. The subgrain rotation mechanism should thus form the basis of any more realistic stress/grain size model, but, unfortunately, little is known about the details of the mechanism, especially in the early stages of recrystallization. TEM examination of dynamically recovered minerals shows that the stable subgrain size is several times smaller than the optically visible "subgrains" that appear to rotate to form recrystallized nuclei. Until the relationship between the two subgrain sizes is understood, and the role that the smaller subgrains play in recrystallization has been elucidated, the stress/grain size relationship cannot be substantially improved.

The final problem concerning the application of any model of dynamically recrystallized grain size versus stress is how the grain size tracks a potentially complicated stress history. It seems reasonable to assume that during the bulk of the strain history of a QP-mylonite zone, the magnitude of the shear stress is relatively constant. However, it is possible for the grain size to adjust late in the zone history to either 1) a slowly waning stress or 2) a hydrostatic condition at elevated temperatures. In both cases, the stress inferred from recrystallized grain size will underestimate the steady state flow stress responsible for the bulk of the movement. It is impossible to estimate the rate at which stress magnitudes decrease at the end of a particular deformation phase, but the experiments of Ross (1977) on olivine suggest that grain size increases rapidly in response to decreasing flow stress, and this is a potentially serious problem of unknown magnitude. The problem of static grain growth at shear stresses below that required for dislocation flow has been discussed by Twiss (1977). However, we believe that the following microstructural criteria are inconsistent with significant static grain growth:

(i) Strongly deformed relics of original grains are commonly found surrounded by essentially strain-free recrystallized grains in mylonites. The driving force for static recrystallization of the deformed relic would be significantly greater than that for grain growth in the recrystallized matrix, and should therefore precede such grain growth.

(ii) TEM examination of dynamically recrystallized grains in mylonites shows that they have a low to moderate density of dislocations, particularly near their boundaries (White, 1976). Retention of these dislocations is inconsistent with significant migration of the recrystallized grain boundaries.

(iii) During annealing the primary recrystallized grain size will decrease with increasing strain, whereas it was found to be independent of strain in **most of** the zones studied here.

(iv) Static grain growth in a primary recrystallized aggregate is characterized by selected growth of individuals and the development of irregular grain shapes, neither of which is seen in even the coarsest of these rocks.

In summary, the miss model for relating stress to recrystallized grain size contains some minor inconsistencies and likely sources of error, but it provides a good fit to the available experimental data, and until a model based on realistic recrystallization mechanism is developed, it is the best available. The only empirical relationship for quartz (Mercier *et al.*, 1977) is based on experiments at unrealistically high pressures, in which measured stresses are subject to significant error. They were also carried out under "wet", but uncontrolled $a_{\text{H}_2\text{O}}$ conditions (Parrish *et al.*, 1976).

Discussion of Calculated Stress Magnitudes

Differential stress magnitudes have been calculated from the recrystallized grain size data using the ~~tw~~ theoretical equations for quartz and feldspar, and the Mercier empirical formula for quartz. The calculated stresses are tabulated in appendix 2, and summarised in figure 21, which uses the stress values derived from the miss equation for quartz. We shall use these values in the following discussion rather than the empirical values, primarily because the experiments (which were designed for quite another purpose) lacked control over some of the important variables.

The calculated stress magnitudes fall into two main groups (fig. 21). The regionally foliated granites (Wyangala, Wondalga and coarser grain sizes at Crackenback) give lower values, generally in the range 20 to 40 MPa. In contrast, most of the mylonites within discrete zones produce stress magnitudes between 60 and 150 MPa. The data from the Woodroffe and Davenport thrusts span both ranges.

The difficulty in interpreting these stress values is clear from the Woodroffe and Davenport thrust data. There is a close correlation between calculated stress and rock composition (esp. degree of hydration) and there is no correlation between stress and position with respect to the two thrust planes. It thus seems that the variation in recrystallized grain size in this case is merely reflecting the effect of H_2O on the rheology of quartz and feldspar. The data from the granitic rocks of the Lachlan fold belt, however, are much more consistent with expected stress variations. Three distinct groups of stresses are found in the Crackenback data. The lowest values (around 20 MPa) are recorded in the weakly to moderately deformed granite that makes up the bulk of the intrusion, increasing to about 40 MPa in discrete mylonite zones. Both of these are overprinted by a "higher stress" (80 MPa) event apparently associated with the macroscopic faulting.

The quartz mylonites of the Atnarpa area were specifically chosen for this study because the thrust pile had been mapped in some detail. It thus seemed possible to provide some constraint on the stress magnitudes calculated from grain size by dynamic modelling of the geometry to the thrust sheets. However, the geology is more complex than first appeared and there are insufficient data to pursue this approach. Nevertheless, the calculated stresses do broadly reflect depth within the thrust complex, although the highest stresses are recorded in the upper levels. This is inconsistent with a simple frictional model, but may result directly from the effect

of a higher fluid pressure at depth on frictional resistance (Hubbert and Rubey, 1959), or indirectly through a hydrolytic weakening process.

When all of the data from the Amadeus Basin locality are compared, there is a general picture of increasing stress with increasing dip of the fault zone. According to the model for formation of the thrust nappes (Forman, 1971; Marjoribanks, 1974), this indicates increasing depth of deformation and/or closer proximity to the root zone, both of which may be expected to result in higher stresses.

Given that problems exist in applying the calculated stress magnitudes to specific mylonite zones or groups of zones, it is nevertheless instructive to compare the range of values with crustal stress magnitudes derived from other sources. McGarr and Gay (1979) have recently reviewed the "direct" measurements of stress in the upper parts of the crust using techniques such as overcoring and hydrofracture. Even though the deepest measurement is at only 5 km from the surface, there is some evidence that stress magnitudes are levelling off at 20 to 40 MPa below about 2 to 3 km. This value is remarkably consistent with the data from the regionally foliated granites, which presumably reflect the effects of "normal" orogenic stresses. It is also significant that the highest values recorded in this study (approx. 100 MPa) are somewhat lower than the widely quoted values for frictional shear resistance during stick-slip on a range of discontinuities. If the calculated stresses are realistic, this means either that 1) the laboratory experiments have so far been unable to reproduce the conditions within seismogenic fault zones (e.g., the role of a fluid phase in diffusional processes), or 2) the stresses in the QP regime are lower than in the seismogenic regime.

CONCLUSIONS

(i) The concept of a steady state recrystallized grainsize during deformation of a single phase aggregate by dislocation creep has been shown to apply to a wide variety of deformed rocks. In most mylonite zones studied, this grainsize is strikingly independent of finite strain, although it may not be uniquely related to stress. In particular, it is very sensitive to the water content of the rocks, presumably through a hydrolytic weakening process, and may be less sensitive to temperature. Figure 22 a, however, shows an example of recrystallized grainsize variation that is consistent with a stress concentration between two rigid feldspar grains in a mylonitized granite.

(ii) The Twiss (1977) model for relating subgrain and recrystallized grainsize to differential stress predicts stress magnitudes that are broadly consistent with other constraints, but it has some obvious deficiencies. First, it contains no direct reference to the effects of impurities (esp. hydrous species) or temperature (except through minor temperature dependence of elastic parameters and dislocation Burgers vectors). Second, it does not predict the large difference in grainsize (3 to 5 times) between quartz and feldspar in the same rock, and finally, the model used for recrystallized grains contains some inconsistencies.

(iii) A stress/grainsize relationship based either on a realistic model of recrystallization mechanisms (including the effect of recovery based hydrolytic weakening), or on a range of careful deformation experiments is a potentially powerful tool for determining palaeostress magnitudes.

The constancy of grainsize within most mylonite zones and the ease with which accurate grainsize measurements can be made emphasise the usefulness of such a relationship.

(iv) The most serious practical restriction to applying an improved stress/grainsize relationship is the need to measure grainsize only in single phase aggregates. Rocks that contain more than one phase intermixed on the scale of the recrystallized grains are unsuitable for grainsize measurement.

(v) Differential stress magnitudes calculated from the Twiss stress/grainsize equation for quartz are consistent with general crustal stress levels of a few tens of MPa, rising to the order of 100 MPa in mylonite zones.

(vi) We have found no consistent difference in stress between mylonite zones of quite different geometries and tectonic settings, except for a possible decrease in stress with increase depth (temperature). In the lower temperature regime (200-300°C), fault ranging from horizontal to vertical, and having a variety of displacement vectors all give stresses between 60 and 150 MPa.

ACKNOWLEDGEMENTS

This work has been supported by research grant no. 14-08-001-14845 from the U.S. Geological Survey. We have benefitted considerably from discussions with Bruce Hobbs, Tim Bell and Rob Twiss, and are most grateful to the Geology departments of the Universities of Adelaide and Sydney, as well as Tim Bell and Bruce Hobbs for access to thin section and rock collections.

APPENDIX 1 - MEASUREMENT OF RECRYSTALLIZED GRAINSIZE

The most accurate way of obtaining grain size from a thin section is to measure the intercepts that the grains make with a random straight line. Papers by Exner (1972) and Pickering (1976) outline the theory behind these measurements and show that for equi-sized spheres the mean diameter (\bar{d}) of the grains is related to the mean linear intercept (\bar{l}) by the following relation:

$$\bar{d} = 1.5 \times \bar{l}$$

The accuracy of the measurements can be determined from the standard deviation of the mean linear intercept:

$$= \frac{\sigma_d}{\sqrt{n}}$$

where σ_d = standard deviation of individual intercept lengths

n = number of grains counted

(Blank & Gladman, 1970)

Using experimental data and the above equation it can be shown that the relative error of the mean linear intercept is:

$$\frac{\sigma_d}{\bar{d}} = \frac{0.7}{\sqrt{n}}$$

(Pickering, 1976)

In order to obtain a relative error of 2.2% 1000 grains must be measured.

Initially measurements were made on a square grid placed over a photomicrograph of the specimen, enabling an accurate analysis of one small area. The data obtained in this way approximate a log normal distribution. An alternative method of measurement is to count intercepts along a grid line of known length in the eyepiece of the microscope. Comparison of the two methods shows that the direct microscope measurement is faster than the photographic technique and it has much the same accuracy. The second method also enables a more representative sampling of the thin sections, and ambiguities regarding position of grain boundaries are more easily resolved.

Where possible, measurements were made, both parallel and perpendicular to the trace of the rock foliation, on each of the perpendicular sections cut at right angles to the foliation and orthogonal with any mineral lineation. This gives the three principal axes of the grains, assuming the grain shape to be ellipsoidal. A single measurement for grain diameter was obtained by calculating the diameter of the sphere equal volume to the ellipsoid. This value is not very different to that obtained by simply averaging the lengths of the three principal axes, and in cases where all three values were not known, then an arithmetic mean was used for the grain diameter.

In all cases, measurements were only made in areas of the thin section that are monomineralic or very nearly so. Some of the Heavitree

Quartzites contain appreciable fine muscovite and chlorite and are unsuitable for measurement, but the grainsize is very little affected by layer silicate contents of less than about 2% (fig.22 a,b). The more intensely deformed felsic rocks are characterized by a mineralogical homogenization, producing ultimately a uniform slaty or phyllitic rock (cf. Bell and Etheridge, 1973, 1976). Such rocks are unsuitable for recrystallized grainsize measurement.

Sample No.	Thickness	Locality
74-1477	41	Locality A
74-1478	42	
74-1479	43	
74-1481	44	
74-1482	45	
74-1483	46	
74-1484	47	
74-1484	48	
20932	73	Locality B
20933	74	
20934	75	
20935	76	
20936	77	
20937	78	
20938	79	
20939	80	
20940	81	
20941	82	
20942	83	Locality C
20943	84	
20944	85	
20945	86	
20946	87	
20947	88	Locality D
20948	89	
20949	90	
20950	91	
20951	92	
20952	93	
20953	94	
20954	95	
20955	96	
20956	97	
20957	98	Locality E
20958	99	
20959	100	
20960	101	
20961	102	

APPENDIX 2 -- DIFFERENTIAL STRESS MAGNITUDES CALCULATED FROM TWISS EQUATION

Stress values from the Heavitree Quartzite - Atnarpa area (MPa).

Locality	Sample No.	Quartz	
		Twiss	Mercier
Locality A	74-1477	47	23
	74-1478	45	22
	74-1479	41	20
	74-1481	45	22
	74-1482	45	22
	74-1483	52	26
	74-1484	47	24
Locality B	50932	73	37
	50933	67	34
	50934	79	40
	50935	74	38
	50936	72	37
	50937	65	33
	50938	71	36
	50939	71	36
	50940	68	35
	50942	63	32
	50943	55	28
	50944	55	27
Locality C	50945	60	30
	50948	69	35
	50951	58	29
	50954	60	30
	50958	47	23
Locality D	50962	49	25
	50963	46	23
	50964	51	26
	50965	52	26
	50966	48	25
	50967	49	24
	50968	49	25
	50969	48	24
	50970	48	24
50971	50	25	
Locality E	50986	143	75
	50983	131	69
	50992	138	73
	50996	159	84
	50988	161	85
	50991	63	32

Stress values from central Australian Quartzites (MPa).

Locality	Sample No.	Quartz	
		Twiss	Mercier
Damper Gorge.	50912	90	47
	50913	99	53
	50914	86	45
	50916	76	40
	50917	87	45
	50918	80	41
	50919	92	49
	50920	87	45
	50921	84	44
	50922	87	45
	50924	73	37
	50925	102	53
	50926	77	40
	50927	80	42
	50928	78	41
	50929	89	47
50930	71	36	
Ormiston Gorge South	74-1486	127	66
	74-1487	111	58
	74-1488	126	66
	74-1489	131	68
	74-1490	119	62
	74-1498	124	65
	74-1499	116	60
	74-1503	121	63
	74-1505	122	64
	74-1506	109	57
Chewings Range Quartzite-Fish Hole	74-1473	169	86
	74-1472	138	74
	74-1471	124	65
	74-1470	179	95
	74-1409	145	79
	74-1468	140	74
	74-1476	146	79

Stress values from the Musgrave - Mann ranges (MPa).

Locality	Sample NO.	Quartz		Feldspar
		Twiss	Mercier	
Woodroffe Thrust.	Gi	140	74	
	G3a	87	45	316
	G3b	75	38	279
	G3c	73	37	279
	G4	69	35	229
	G5	46	23	212
	A5	37	18	98
	A4	30	15	115
	A3	24	12	93
	A4	34	17	115
	A1	41	21	157
Davenport Shear.	16	27	13	112
	18	18	9	73
	400	29	14	-
	917	28	14	100
	318	41	23	119
	323	39	19	103
	472	35	17	-
	537	51	26	185
	611	36	18	-
	620	35	17	119
	673	40	20	-
	882	39	19	127
	917a	33	16	106
	917b	32	16	103
	917	33	16	115
	9171	35	17	112
	917p	42	35	132
	940	40	20	137
	948b	37	20	157
	948	32	16	123
	948	45	23	-
	948i	47	23	185
	531	65	33	165
	543	50	25	-
	689	50	25	-
	698	58	30	185
	783	49	25	-
	788	50	25	-
	900	48	24	174
	907b	62	32	212
	907f	58	30	-
	911	52	26	174
	917s	47	23	174
928g	73	40	-	
928h	102	53	165	

Stress values from eastern Australian foliated granites (ma)

Locality	Sample No.	Orientation		Feldspar
		Twiss	Mercier	
Wyangala Gneiss	34697	29	14	
	34710	41	20	
	34711	38	19	
	34712	35	17	
	34714	38	19	
	34718	35	17	
	34719	37	18	
	34720	35	17	
	34721	34	17	
	34727	21	10	
	34729	23	11	
	34743	21	10	
	34744	23	11	
	34799	31	15	
	5701-213	33	16	
	5206-214	26	13	
	WYO	40	20	
	WY10	40	20	
	WY16	39	19	
	WY30	40	20	
WY35	40	20		
Wondalga Gneiss	50231	26	13	143
	50232	28	14	108
	50234	24	11	101
	50235	23	11	-
	50236	28	14	108
	50244	45	22	133
	50245	27	13	133
	50246	28	13	114
	50247	43	21	-
	41255	30	15	111
	41277	36	19	71
	41278	24	11	106
	41279	17	8	87
	41309	17	8	83
	41310	16	8	79
	47360	30	15	-
	47361	50	27	-
	47362	33	16	187
	47363	33	16	198
	47364	34	17	133
	47365	30	15	114
	47372	44	22	-
	49634	28	13	-
	49625	31	15	-
	49639	29	14	178
	49646	36	18	-
	49679	37	18	129
49684	27	13	138	

Stress values from eastern Australian fault zones (MPa).

Locality	Sample No.	Coarse Quartz		Fine Quartz		Feldspar
		miss	Mercier	Twiss	Mercier	
Crackenback fault - Mt. Kosciusko	51108	28	14	90	46	174
	51110	28	14	55	28	148
	51111	26	13	80	41	-
	51114	29	14	-	-	130
	51115	34	17	-	-	164
	51116	27	13	32	33	160
	51117	26	13	80	41	-
	51119	28	14	75	38	-
	51121	24	12	82	42	-
	51123	29	14	-	-	138
	51128	22	10	-	-	65
	51131	22	11	-	-	74
	51135	24	11	88	46	-
	51142	31	16	-	-	125
	51144	22	11	-	-	123
	51145	21	10	91	47	97
	51147	22	11	-	-	114
	51149	14	7	-	-	101
	51152	34	17	-	-	99
	51153	37	19	-	-	-
51157	32	16	-	-	143	
51158	41	20	-	-	114	
51161	14	7	-	-	-	
51168	41	20	-	-	124	

Locality	Sample No.	Quartz		Feldspar
		Twiss	Mercier	
Coolac Serpentine Belt	88021	106	55	
	38022	131	69	
	38023	163	86	
	38024	131	69	
	41195	150	79	
	41196	150	79	
	41197	150	75	
	37661	79	41	
	37679	51	26	
	37685	58	30	157
	37904	472	94	49

REFERENCES

- Ashley, P.M., Chenhall, B.E., 1976. Mylonitic rocks in the Young Granodiorite, Southern New South Wales. 3. and Proc. Roy. Soc. N.S.W., 109: 25-33.
- Ashley, P.M., Chenhall, B.E., Cremer, P.L., Irving, A.J., 1971. The geology of the Coolac Serpentinite and adjacent rocks east of Tumut, N.S.W. Proc. Roy. Soc. N.S.W., 104: 11-20.
- Bell, T.H., 1978. Progressive deformation and re-orientation of fold axes in a ductile mylonite zone. The Woodroffe Thrust. Tectonophysics, 44: 285-320.
- Bell, T.H., Etheridge, M.A., 1973. Microstructure of mylonites and their descriptive terminology. Lithos, 6: 337-348.
- Bell, T.H., Etheridge, M.A., 1976. The deformation and recrystallization of quartz in a mylonite zone, central Australia. Tectonophysics, 32: 235-267.
- Bird, J.E., Mukherjee, A.K., Dorn, J.E., 1969. Correlations between high-temperature creep behaviour and structure. In: Proceedings of an International Conference, Haifa, Israel: 255-342.
- Blank, J.R., Gladman, T., 1970. Quantitative Metallography. In: Tools and Techniques in physical metallurgy, vol. 1, Weinberg F. (ed.): 265-327.
- Brooks, C., Leggo, M.D., 1972. The local chronology and regional implications of a Rb-Sr investigation of granitic rocks from the Corryong district, southeastern Australia. J. Geol. Soc. Aust., 19: 1-19.
- Chappell, B.W., White, A.J.R., 1974. Two contrasting granite types. Pacific Geology, 8: 173-174.
- Cleary, J.R., Doyle, H.A., Moye, P.G., 1964. Seismic activity in the Snowy Mountains region and its relationship to geological structures. J. Geol. Soc. Aust., 11: 89-106.
- Collerson, K.D., Oliver, R.L., Rutland, R.W.R., 1972. An example of structural and metamorphic relationships in the Musgrave orogenic belt, central Australia. J. Geol. Soc. Aust., 18: 379-393.
- Douglas, J.G., Ferguson, J.A., 1976. Geology of Victoria. Geol. Soc. Aust. Special Publ. 5, pp. 528.
- Escher, A., Watterson, J., 1974. Stretching fabrics, folds and crustal shortening. Tectonophysics, 22: 223-231.
- Evernden, J.F., Richards, J.R., 1962. Potassium-Argon ages in eastern Australia. J. Geol. Soc. Aust., 9: 1-50.
- Exner, H.E., 1972. Analysis of grain- and particle-size distribution in metallic materials. Int. Met. Reviews, Review 159, 17: 25-42.

- Forman, D.J., 1971. The Arltunga Nappe Complex, MacDonnell Ranges, N.T., Australia. *Jour. Geol. Soc. Aust.*, 18: 172-182.
- Goetze, C., 1975. Sheared Iherzolites: From the point of view of rock mechanics. *Geology*, 3: 172-173.
- Golding, H.G., 1969. The Coolac-Goobarragandra Ultramafic Belt, N.S.W. *J. and Proc. Roy. Soc. N.S.W.*, 102: 173-187.
- Hobbs, B.E., 1965. Structural analysis of the rocks between the Wyangala Batholith and the Copperhanna Thrust, New South Wales. *Geol. Soc. Aust. J.*, 12: 1-24.
- Hobbs, B.E., 1966. Microfabric of tectonites from the Wyangala Dam area, New South Wales, Australia. *Geol. Soc. Am. Bull.*, 77: 685-706.
- Hobbs, B.E., 1969. Recrystallization of single crystals of quartz. *Tectonophysics*, 6: 353-401.
- Hobbs, B.E., McLaren, A.C., Paterson, M.S., 1972. Plasticity of single crystals of synthetic quartz. In: *Flow and Fracture of Rocks*, Heard, H.C., Borg, I.Y., Carter, N.I., Raleigh, C.B., (eds.). *Am. Geophys. Union, Geophys. Monograph Ser.* 16: 29-53.
- Kolstadt, D.L., Goetze, C., 1974. Low stress high temperature creep in olivine single crystals. *J. Geophys. Res.*, 79: 2045-2051.
- Major, R.B., Johnson, J.E., Laeson, B., Mirams, R.C., 1967. Woodroffe 1:250,000 geological map. *Mines Dept. Geol. Survey South Aust.*
- Marjoribanks, R.W., 1974. The structural and metamorphic geology of the Ormiston region, central Australia. *Ph.D Thesis, A.N.U.* (unpubl.), pp 312.
- Marjoribanks, R.W., 1976. The relationship between microfabric and strain in a progressively deformed sequence from central Australia. *Tectonophysics*, 32: 269-293.
- McGarr, A., Gay, N.C., 1978. State of stress in the earths crust. *Ann. Rev. Earth Plan. Sci.*, 6.
- Mercier, J-C.C., Anderson, D.A., Carter, N.L., 1977. Stress in the Lithosphere: Inference from steady state flow of rocks. *Pure Appl. Geophys.*, 115.
- Packham, G.H. (ed.), 1969. The geology of New South Wales. *J. Geol. Soc. Aust.*, 16, pp 654.
- Parrish, D.K., Kriuz, A., Carter, N.L., 1976. Finite element folds of similar geometry. *Tectonophysics*, 32: 183-207.
- Pickering, F.B., 1976. The basis of quantitative metallography. *Metals and Metallurgy Trust for the Inst. of Metallurgical Technicians*, London, pp 38.

- Poirier, J.P., Nicolas, A., 1975. Deformation - induced recrystallization by progressive misorientation of subgrain - boundaries, with special reference to mantle peridotites. *J. Geology*, 83: 707-720.
- Raleigh, C.B., and Kirby, S.H., 1970. Creep in the upper mantle. *Min. Soc. Am. Special paper 3*: 113-121.
- Ross, J.V., Ave Lallement, H.G., Carter, N.L., 1977. Neoblast and sub-grain sizes in experimentally deformed olivine. *EOS*, 58: 512.
- Rutland, R.W.R., 1976. Orogenic evolution of Australia. *Earth Sci. Rev.*, 12: 161-196.
- Scheibner, E., 1974a. Lachlan Fold Belt. Definition and review of structural elements. In: Markham, N.L., Basden, H. (eds.): *The mineral deposits of New South Wales*, Geol. SUN. N.S.W., Sydney: 108-113.
- Scheibner, E., 1974b. Tectonic map of New South Wales, scale 1:1,000,000. *Geol. Surv. N.S.W.*, Sydney.
- Sibson, R.H., 1977. Fault rocks and fault mechanisms. *J. Geol. Soc. Lond.*, 133: 191-213.
- Solomon, M., Griffiths, J.R., 1972. Tectonic evolution of the Tasman Orogenic zone, eastern Australia. *Nature Phys., Sci.*, 235: 3-6.
- Stewart, A.J., 1971. Potassium - Argon dates from the Arltunga Nappe Complex, Northern Territory. *J. Geol. Soc. Aust.*, 17: 205-211.
- Twiss, R.J., 1977. Theory and applicability of a recrystallized grain-size palaeopiezometer. *Pure Appl. Geophys.*, 115: 227-244.
- Wells, A.T., Forman, D.J., Ranford, L.C., Cook, P.J., 1970. Geology of the Amadeus Basin, central Australia. *B.M.R. Bull.* 100, pp. 221.
- White, A.J.R., Chappell, B.W., Cleary, J.R., 1974. Geological setting and emplacement of some Australian Palaeozoic batholiths and implications for intrusive mechanisms. *Pacific Geology*, 8: 159-171.
- White, A.J.R., Williams, I.S., Chappell, B.W., 1977. Geology of the Berridale 1:100,000 sheet. *Geol. Surv. N.S.W.*, 8625.
- White, S., 1975. Syntectonic recrystallization and texture development in quartz. *Nature Phys. Sci.*, 244: 276-270.
- White, S., 1976. The effect of strain on the microstructures, fabrics and deformation mechanisms in quartzites. *Phil. Trans. Roy. Soc. Lond. A*, 283: 69-86.
- White, S., 1977. Geological significance of recovery and recrystallization processes in quartz. *Tectonophysics*, 39: 143-170.
- Wilson, C.J.L., 1973. The prograde microfabric in a deformed quartzite sequence, Mt. Isa, Australia. *Tectonophysics*, 19: 39-81.
- Var Khan, M., 1972. The structure and microfabric of part of the Arltunga ia. Ph.D Thesis, A.N.U. (unpubl.), pp.103.

TABLE 1. Grainsize data from samples collected in the Musgrave Ranges.

Locality	Sample Number	Grainsize (μm)		Comments
		Quartz	Feldspar	
Woodroffe Thrust	G2	10	-	Granulite Facies ← Thrust Amphibolite Facies
	G3a	20	5	
	G3b	25	6	
	G3c	26	6	
	G4	28	8	
	G5	51	9	
	A5	71	28	
	A4	95	22	
	A3	136	30	
	A2	79	22	
A1	60	14		
Davenport Thrust	16	114	23	1. Adamellite
	18	207	43	
	400	100	-	2. Amph-bi+ga
	917m	105	27	no px.
	318	50	21	3. Amph-ga-bi #hbl±Opx (Transitional facies)
	323	66	26	
	472	76	-	
	474	78	21	
	537	44	11	
	611	75	-	
	620	76	21	
	673	62	-	
	882	65	19	
	917a	85	25	
	917b	89	26	
	917k	83	22	
	917l	78	23	
	917p	58	18	
	940	62	17	
	948b	70	14	
	948d	86	20	
	948g	53	-	
	948c	50	11	
	531	31	13	4. Ga-red bi-Opx (Granulite Facies)
	543	46	-	
	689	46	-	
	698	36	11	
	783	47	-	
	788	45	-	
	900	48	12	
	907b	33	9	
	907f	36	-	
	911	43	12	
	917s	50	12	
	928g	26	-	
	928h	16	13	

TABLE 2. Grainsize data from the foliated granites of eastern Australia.

Locality	Sample number	Grainsize (μm)		Comments
		Quartz	Feldspar	
Wondalga Batholith	50231	113	19	Area 1. (figure 15)
	50232	103	28	
	50234	130	31	
	50235	140	-	
	50236	103	28	
	50244	52	21	
	50245	109	21	
	50246	105	26	
	50247	56	-	
	41255	94	27	Area 2. (figure 15)
	41277	66	51	
	41278	133	29	
	41279	212	38	
	41309	206	41	
	41310	224	44	
	47360	93	-	Area 3. (figure 15)
	47361	45	-	
	47362	81	13	
	47363	83	12	
	47364	79	21	
	47365	92	26	
	47372	54	-	
	49634	106	-	Area 4. (figure 15)
	49635	88	-	
	49639	98	14	
	49646	71	-	
49679	70	22		
49684	111	20		
Wyangala Batholith	34697	101		Bigga Area (figure 16)
	34710	61		
	34711	69		
	34712	78		
	34714	69		
	34718	76		
	34719	71		
	34720	77		
	34721	80		
	34727	163		Binda Area (figure 16)
	34729	139		
	34743	157		
	34744	145		
	34799	91		
	5701-21	85		
	5206-21	121		
	WY0	62		Wyangala Dam Area (figure 16)
	WY10	62		
	WY16	65		
WY30	64			
WY35	64			

Table 3. Grainsize data from discrete fault zones within the eastern Australian Granites - Coolac and Mt. Kosciusko areas.

Locality	Sample Number	Grainsize (µm)		Comments	
		Quartz	cldspar		
Coolac Serpentine Belt.	38021	15		Area 5.	
	38022	10-12		(figure 15)	
	38023	6-10			
	38024	10-12			
	41195	8-10		Area 6.	
	41196	8-10		(figure 15)	
	41197	8-10			
	37661	23			
	37679	44		Area 7.	
	37685	36	14	(figure 15)	
37904	18				
		<u>Coarse</u>	<u>Fine</u>		
Crackenback Fault - Mt. Kosciusko	51108	108	19	10	
	51110	109	40	13	Foliated Granite
	51111	118	23		
	51114	99		16	Mylonite
	51115	81		11	
	51116	112	31	12	
	51117	117	23		
	51119	104	25		Foliated Granite
	51121	132	22		
	51123	99		15	Mylonite
	51131	154		42	
	51135	138	20		Foliated Granite
	51142	89		20	Mylonite
	51144	151		20	
	51145	156	19	29	Foliated Granite
	51147	152		22	
	51149	302		27	
	51152	80		27	
51153	69				
51157	88		16	Mylonite	
51158	61		22		
51161	253			Foliated Granite	
51168	61		20	Mylonite	

LISTING OF FIGURE CAPTIONS

- Figure 1. Map of Australia showing the three main sample localities used in this study. 1) Woodroffe-Davenport thrusts; 2) Thrust nappes of Amadeus Basin; 3) Granites of Lachlan fold belt.
- Figure 2. A generalized geological map of the MacDonnell Ranges (after Wells ~~et al~~, 1970).
- Figure 3. Geological map of the Atnarpa area showing the six sample localities (geology after Yar Khan, 1972).
- Figure 4. Geological map of the Ormiston area showing the two thrusts that were sampled (geology after Marjoribanks, 1974).
- Figure 5. Cross-section through Damper Gorge showing specimen locations and detailed structure.
- Figure 6. Graph summarizing the recrystallized grainsize data from all localities within the Heavitree Quartzite.
- Figure 7. Photomicrographs of Heavitree Quartzite from the Atnarpa area, (a) Totally recrystallized sample from locality A. (b), (c) and (d) three samples from Ruby Gorge (locality B) showing increasing strain in the old grains without any significant variation in recrystallized grainsize. (e) Totally recrystallized sample from adjacent to the thrust at locality B. The grainsize in this sample is larger than in those shown in (a), (b) or (c) (scale = .2mm in all micrographs).
- Figure 8. Optical micrograph at Heavitree Quartzite from the two southern localities at Atnarpa. The first three micrographs show increasing amounts of plastic strain, (a) grains are equidimensional and contain deformation bands and lamellae with very little recrystallization (scale = .3mm), (b) and (c) grains are moderately and highly strained, respectively, and are sitting in a matrix of finely recrystallized quartz (scales = .3mm), (d) Fractures and shear zones (filled with recrystallized quartz), evidence of more brittle deformation (scale = .2mm), (e) The same area as (d) but photographed under plane polarized light. (f) Sample from locality F. The rock is very similar to that shown in (a), little plastic strain and cold worked optical microstructure (scale = .2mm).
- Figure 9. a)-c) Optical micrographs of Heavitree Quartzite from Damper Gorge. There is increasing plastic strain within the original grains and increasing amounts of recrystallization from (a) to (c) and yet the recrystallized grainsize remains constant (scale = .2mm in all micrographs).
d)-f) Optical micrographs of Heavitree Quartzite from Ormiston Gorge. Strain and amount of recrystallization increases from (a) to (c), however there are no samples from this locality that are very highly recrystallized (scale = .2mm in all micrographs).

- Figure 10. Optical micrographs of Chewings Range Quartzite from Fish Hole, showing increasing plastic strain. (a) Quartz grains are only slightly elongate but contain deformation bands (top left hand corner,. There is no recrystallization and the quartz-quartz grain boundaries are serrated. (b) The grains are more highly strained and the bands of recrystallized grains along the grain boundaries indicate some recovery. (c) Ribbon mylonite, even at this high strain there is only a limited amount of recrystallization. (d) Showing relationship between optical subgrains and recrystallized grains. Scale is 0.2 mm in a) to c) , and 0.05 mm in d) .
- Figure 11. Geological map of the Musgrave Ranges showing the location of the sample traverse across the Woodroffe Thrust and the location of the Davenport Thrust (geology after Major et al, 1967).
- Figure 12. Detailed geological map of the Arunta area showing the sample localities adjacent to the Davenport Thrust (geology after Collerson, et al, 1972) .
- Figure 13. Graph of quartz and feldspar recrystallized grainsize variation across the Woodroffe Thrust (sample numbers are given along the horizontal axis). The plot of strain is only approximate and is taken from Bell and Etheridge (1976).
- Figure 14. Map of the granite batholiths outcropping in the Lachlan Fold Belt, eastern Australia. Marked on this figure are the positions of the more detailed sample locality maps.
- Figure 15. Sample locality map for the Wondalga Batholith and the Coolac Serpentine Belt (geology after Brunner et al, 1970).
- Figure 16. Map of the Wyangala Batholith showing sample localities (geology after Brunner et al, 1969).
- Figure 17. Optical micrographs of the Wyangala Granite showing the microstructural changes from a weakly foliated granite to a mylonite. (a) Typical foliated granite, quartz grains show strain shadowing and there is some quartz recrystallization along grain boundaries. (b) Original quartz grains have deformed to long, totally recrystallized ribbons, whereas the feldspars remain unstrained. (c) Total recrystallization of both quartz and feldspar to form a fine grained mylonite (scale = 1 mm in all micrographs).
- Figure 18. Optical micrographs of deformed granites from localized fault zones. (a) Sample from the Goobarragandra River showing a totally recrystallized old grain. The new grains themselves are elongate and a second generation of fine recrystallized grains can be seen along the quartz grain boundaries (scale = .1mm). (b) Moderately deformed granite from the Crackenback area. The quartz grains are highly strained and totally recrystallized, however the feldspars remain undeformed (scale = .3mm). (c) Coarse recrystallized grains in a mylonitized granite from the Crackenback area. The new quartz grains are elongated at about 30° to the main foliation (scale = .3mm).

Figure 19. Geological map of the Crackenback area showing the locations of the samples collected.

Figure 20. Optical micrographs of samples from the granodiorite outcropping at the north-eastern end of the Crackenback River (figure 20). (a) low magnification micrograph showing development of large subgrains in the quartz and fractures radiating out from the boundary of a feldspar grain (scale = .2mm). (b) higher magnification micrograph showing large blocky subgrains and a cross cutting shear zone (scale = .05mm). (c) undulose extinction associated with shear zone (scale = .05mm).

Figure 21. Schematic diagram showing the range of values of stress calculated, using the grainsize/stress equation derived for quartz by Twiss (1977), from the grainsize measurements made in this study.

Figure 22. (a) Optical micrograph of Heavitree Quartzite from locality B in the Atnarpa area. The variation in quartz grainsize is due to a change in the mica content. This variation is seen best in plane polarized light - micrograph (b). (c) Variation in quartz recrystallized grainsize in a sample of Wyangala Granite. The grains decrease in diameter into a local high stress area between two, more rigid, feldspar grains (scale = .2mm in all micrographs).

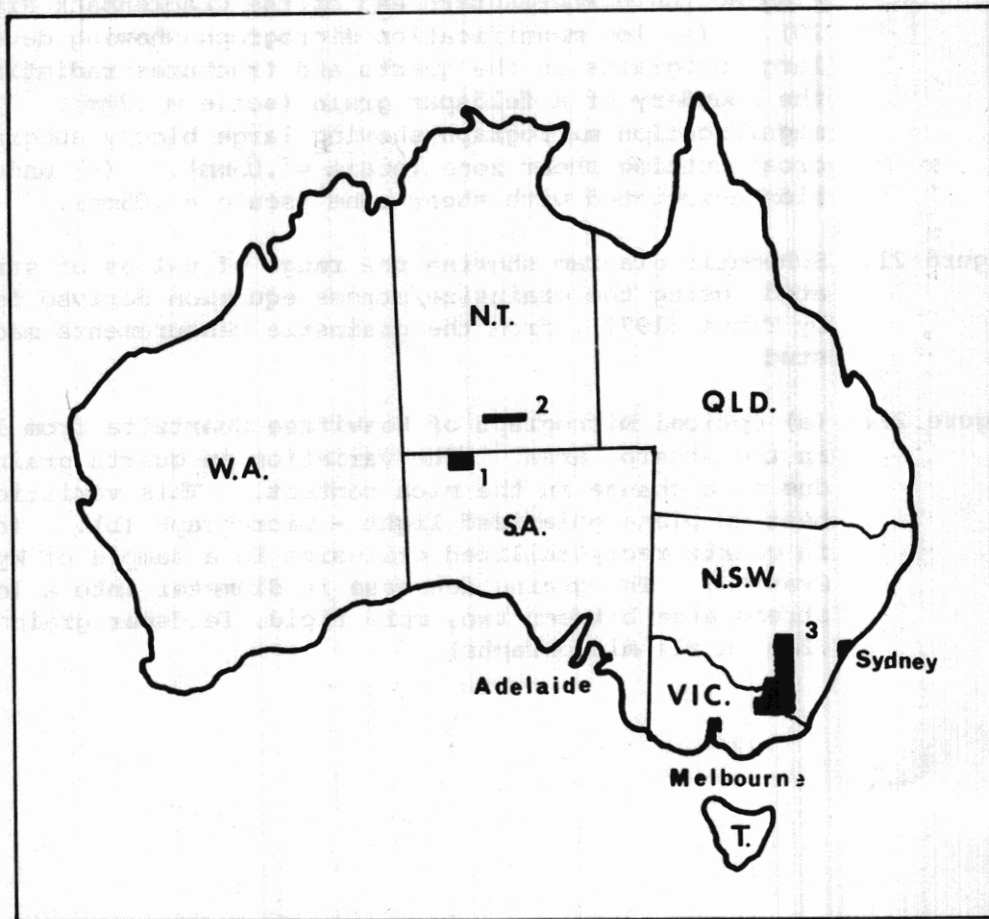


FIGURE 1. Map of Australia showing the 3 main localities sampled during this study.

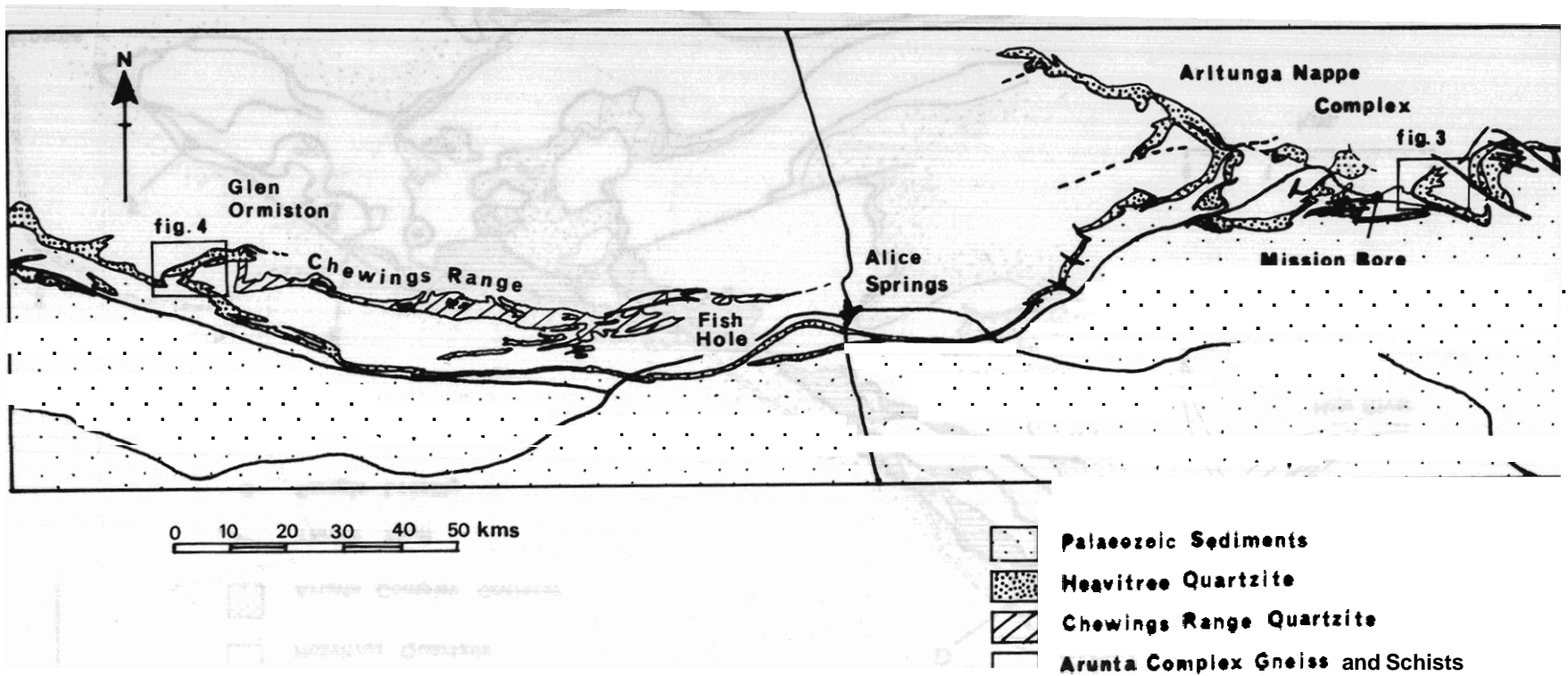


FIGURE 2 Geological map of the MacDonnell Ranges (after Wells et al., 1970)

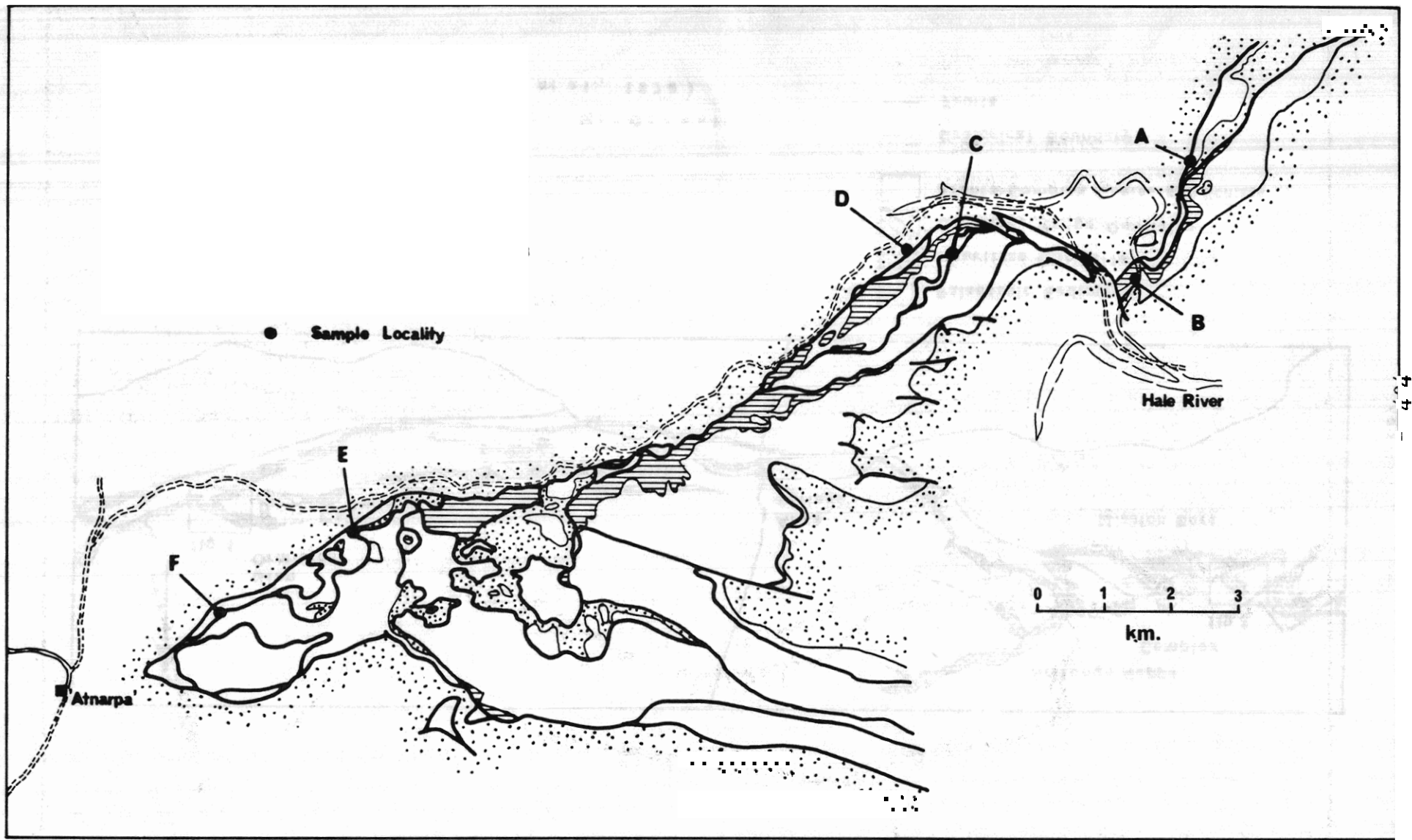


FIGURE 3. Location of Heavitree Quartzite samples from the Atnarpa Area (geology after Yar Khen, 1972)

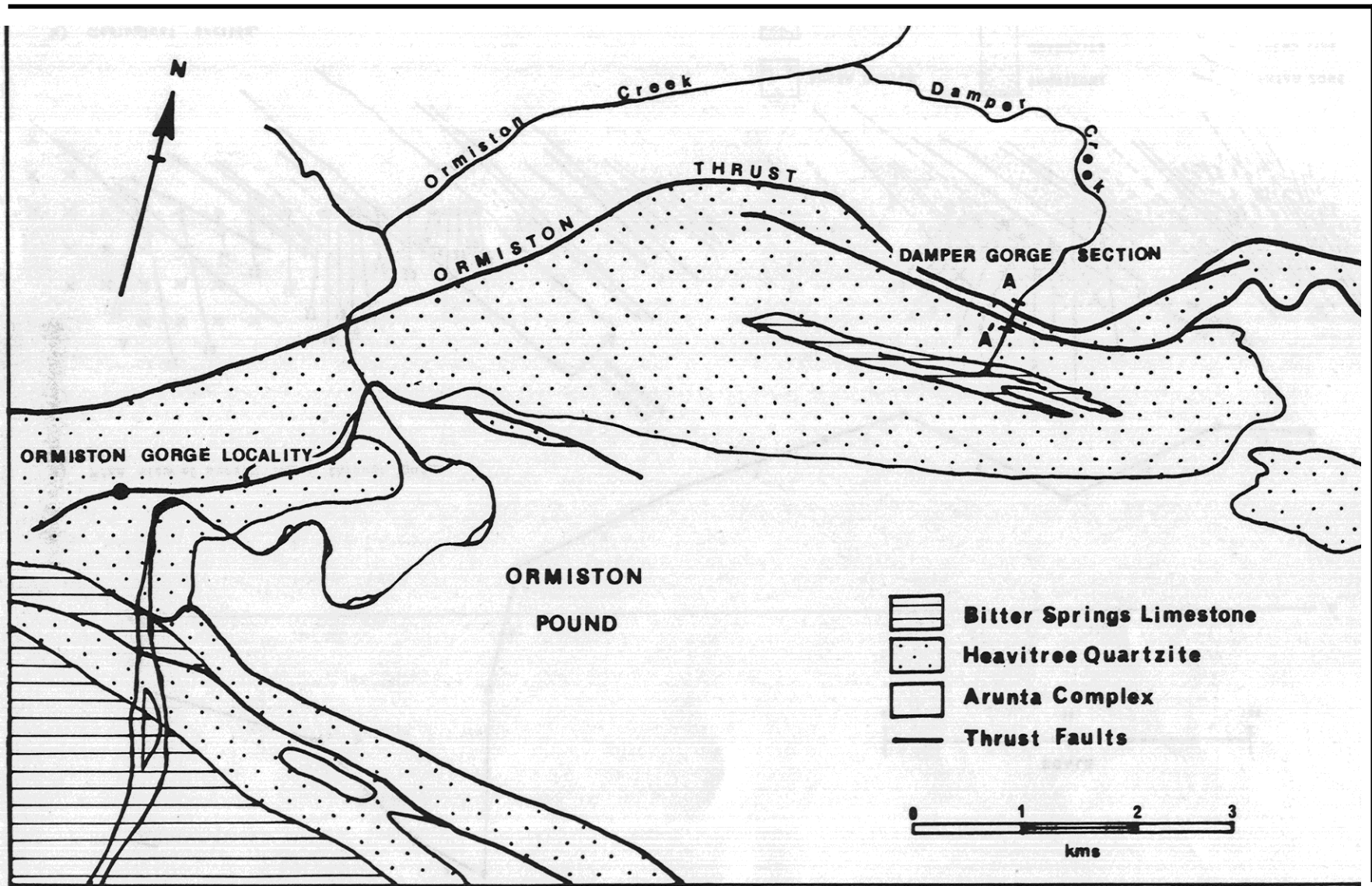


FIGURE 4. Geological map of the Ormiston area showing the major thrusts and the location of sample localities. (Geology after Marjoribanks, 1974)

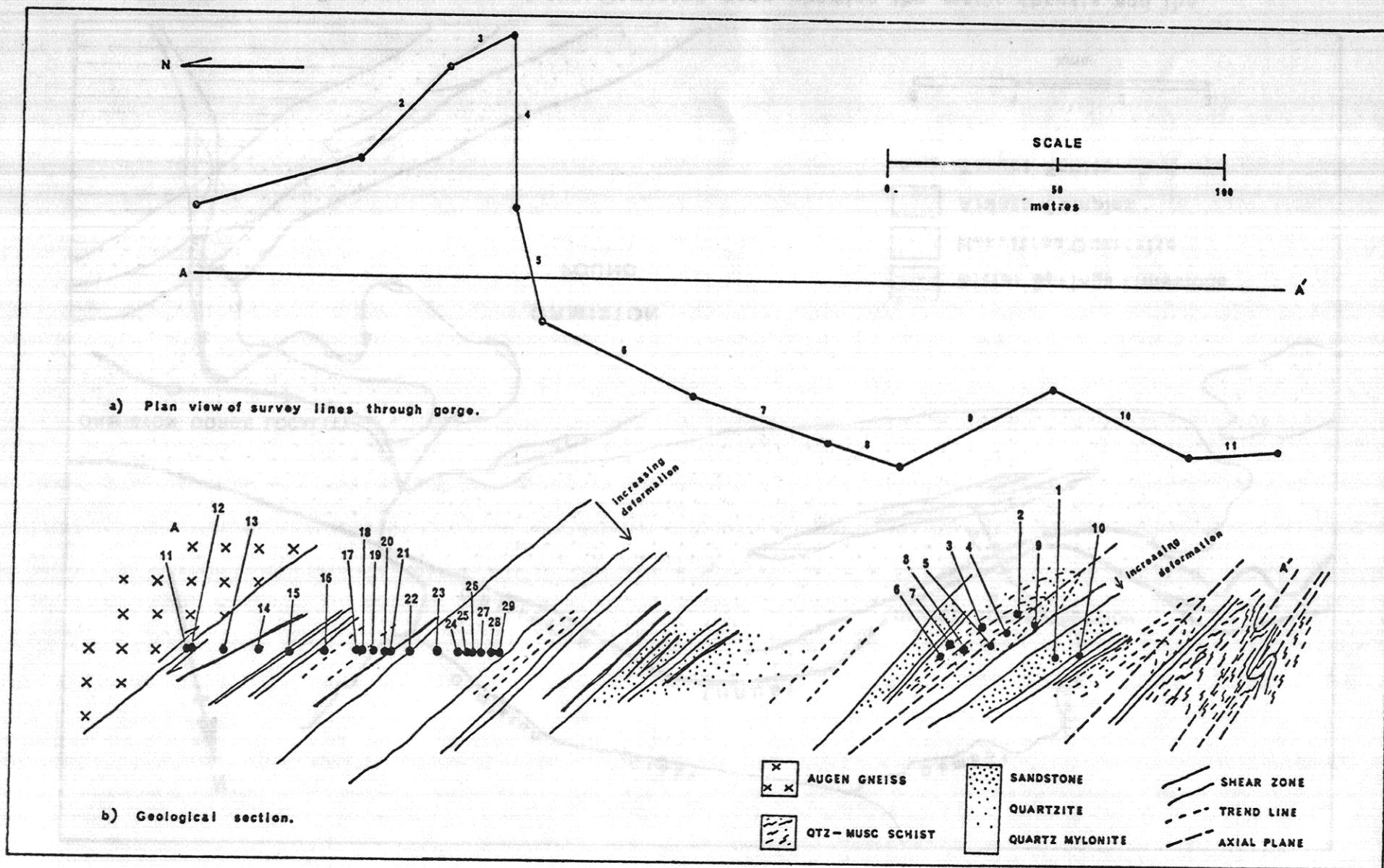
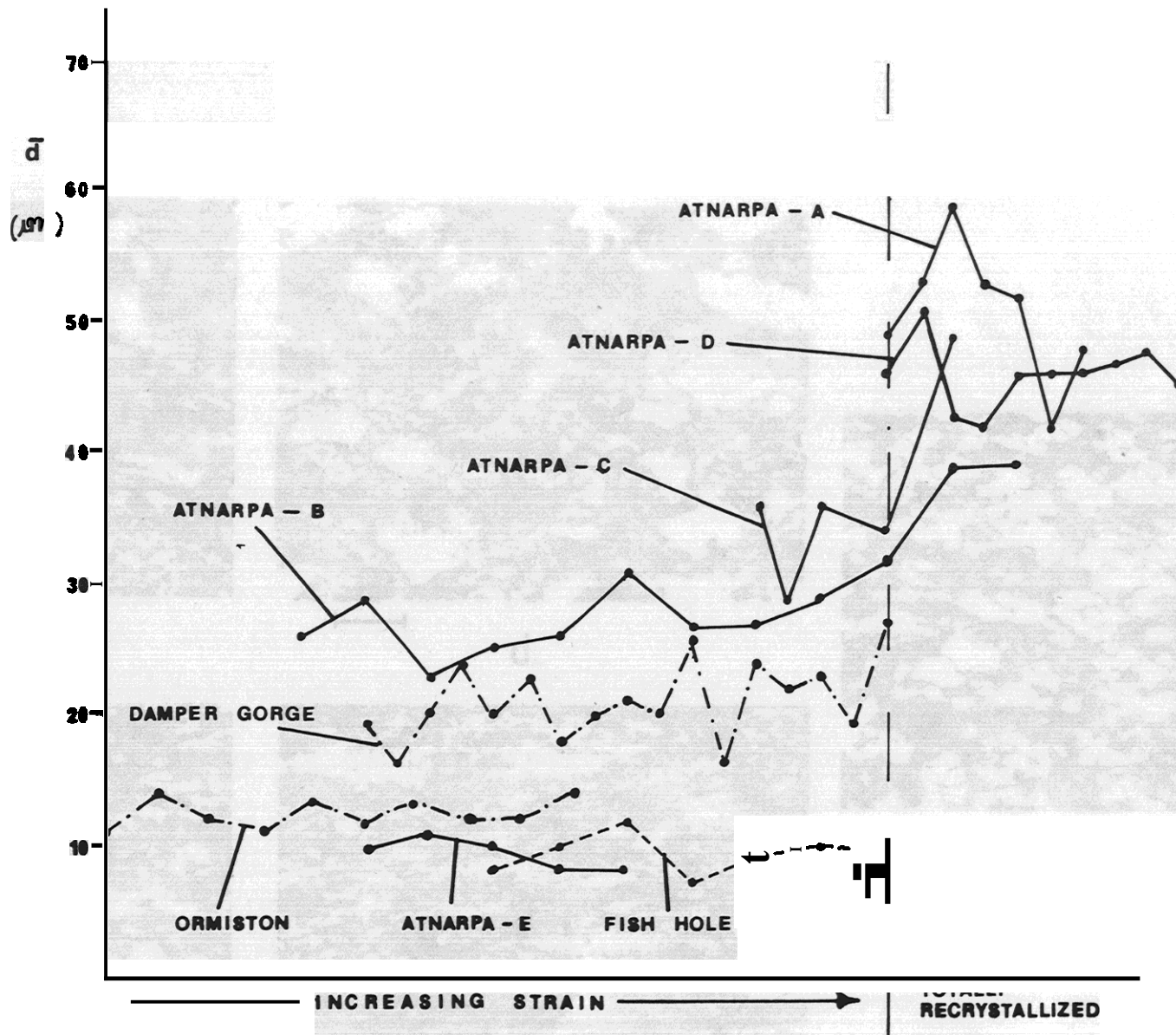
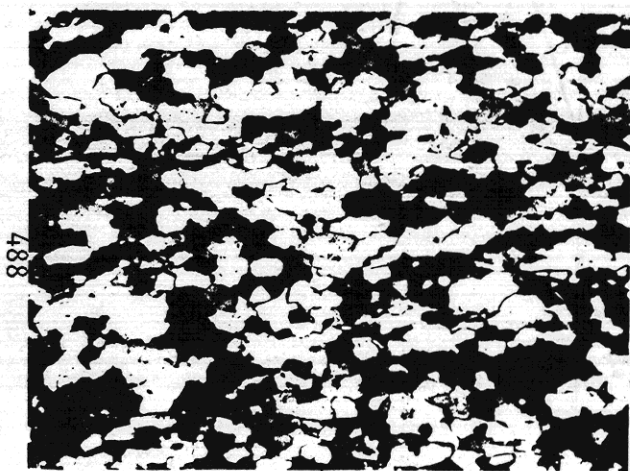
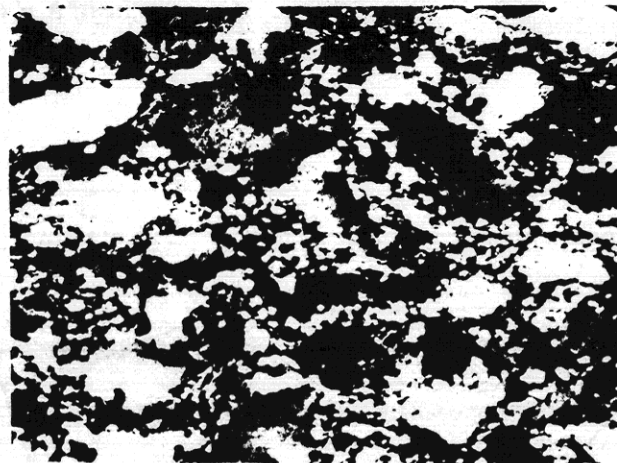


FIGURE 5 PLAN VIEW AND GEOLOGICAL CROSS-SECTION THROUGH DAMPER GORGE, SHOWING SAMPLE LOCALITIES.

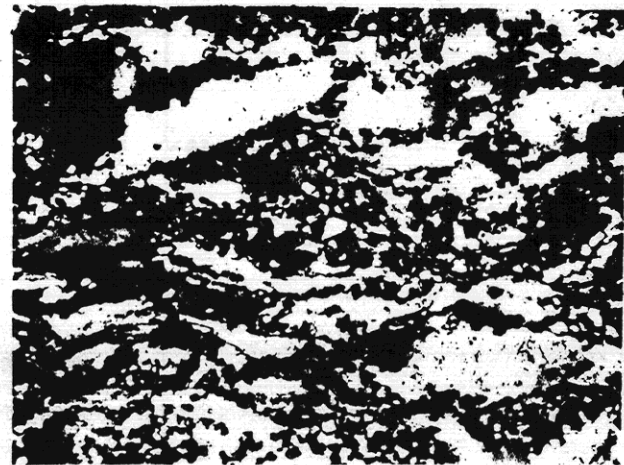




a



b



c



d

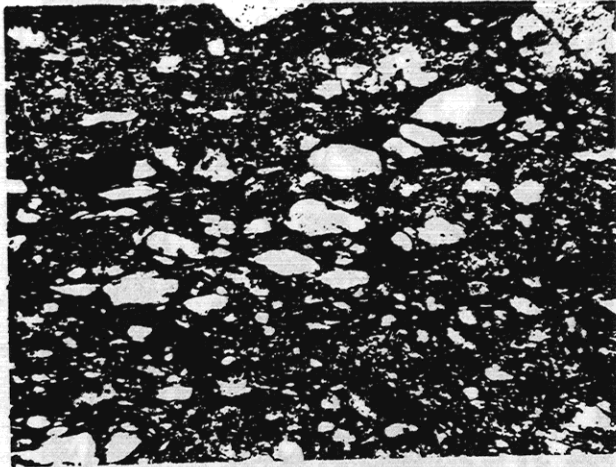


e

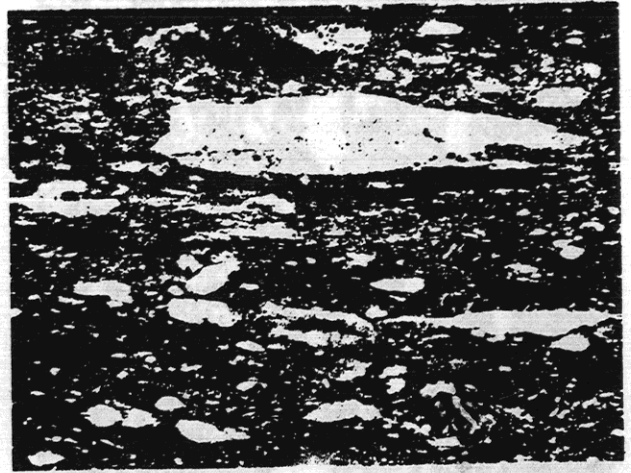
FIGURE 7



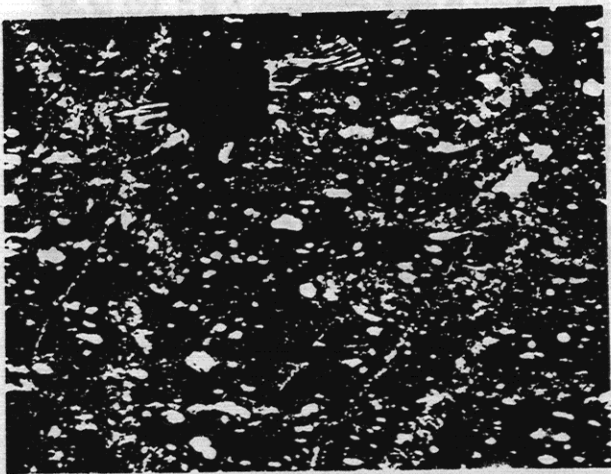
a



b



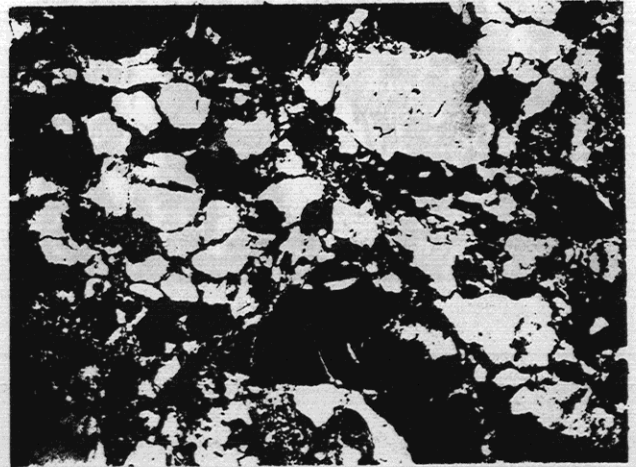
c



d



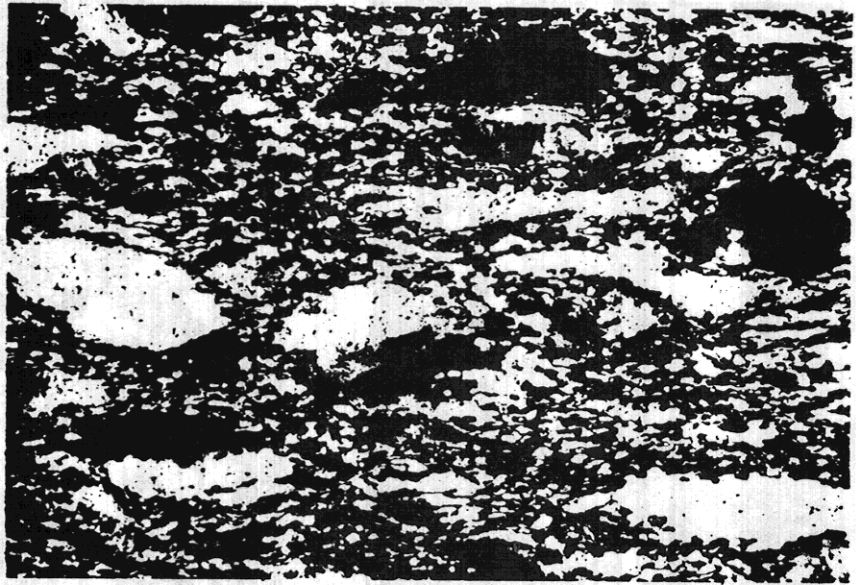
e



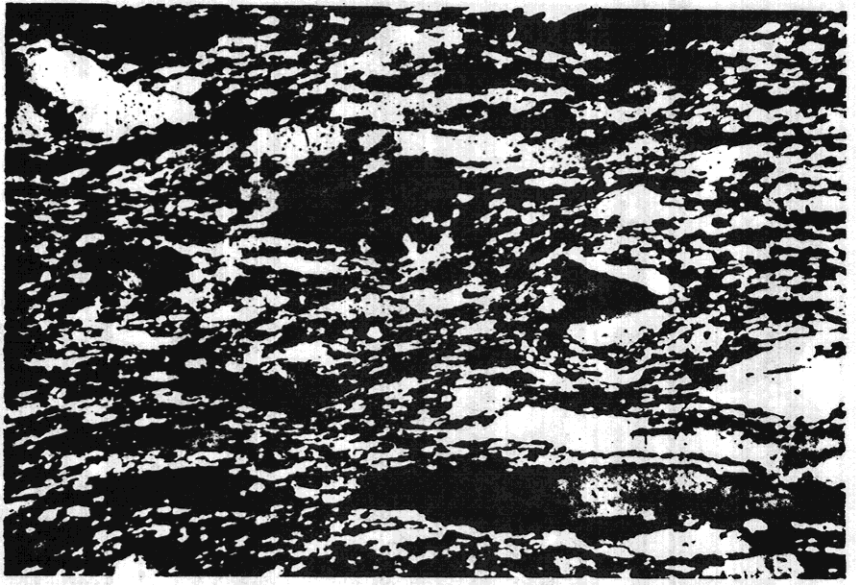
f

FIGURE 8

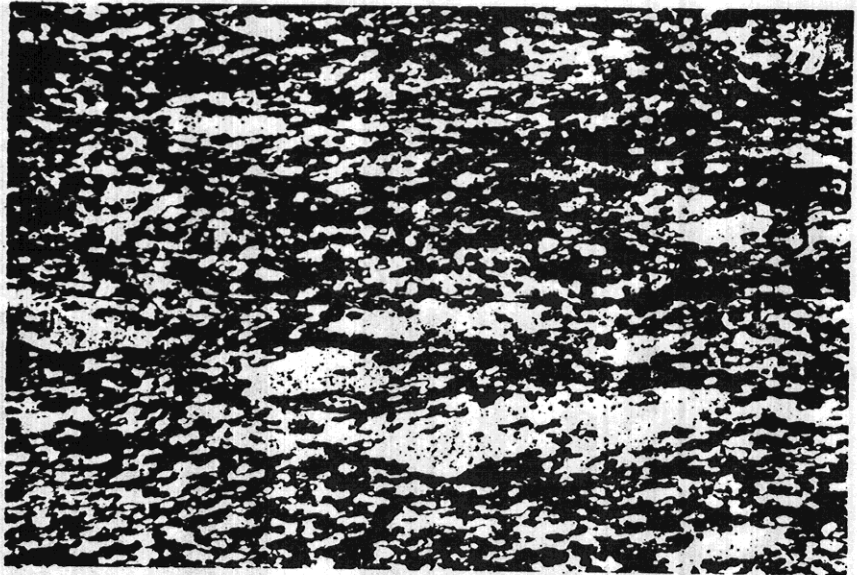
a



b

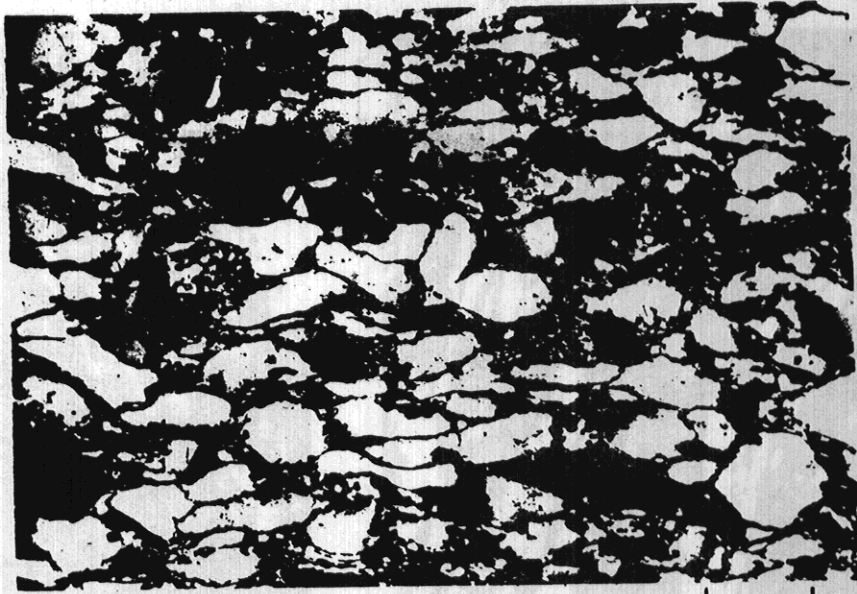


c

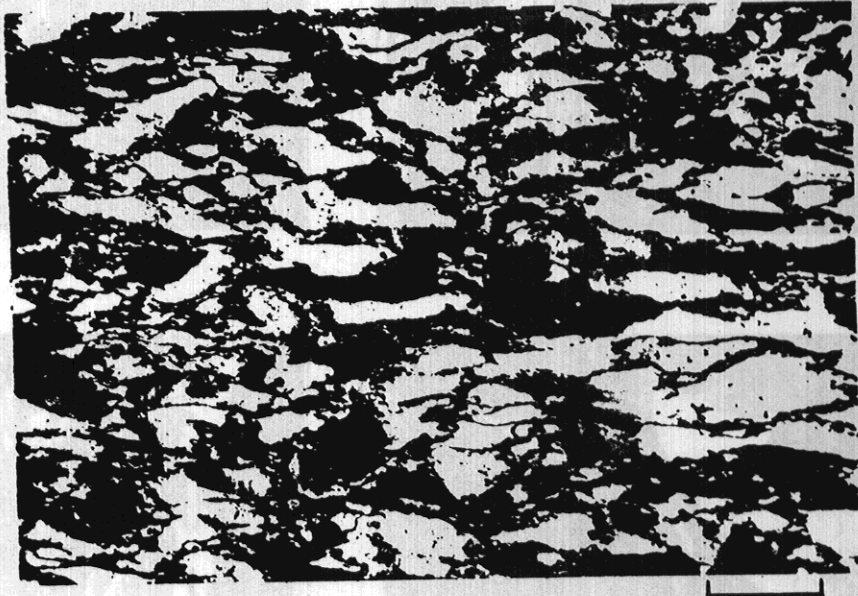


490 FIGURE 9

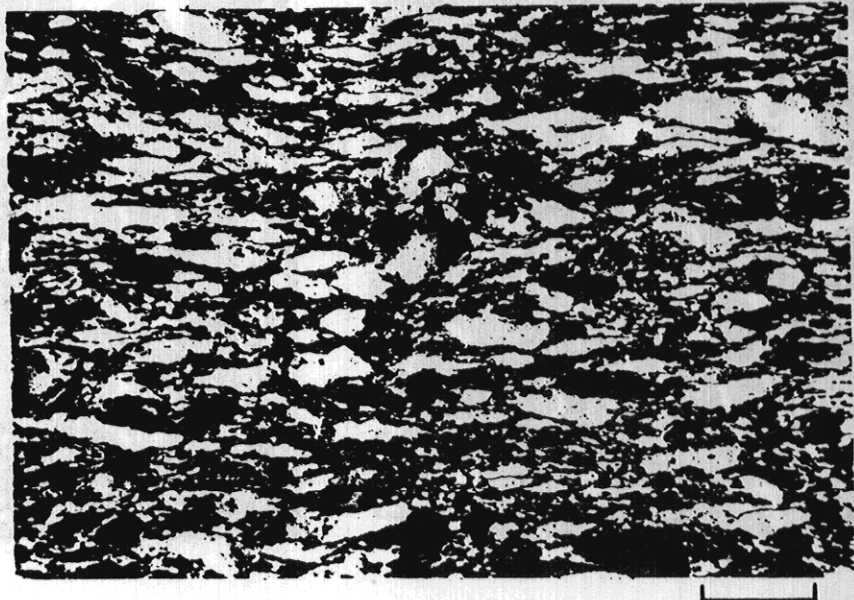
d



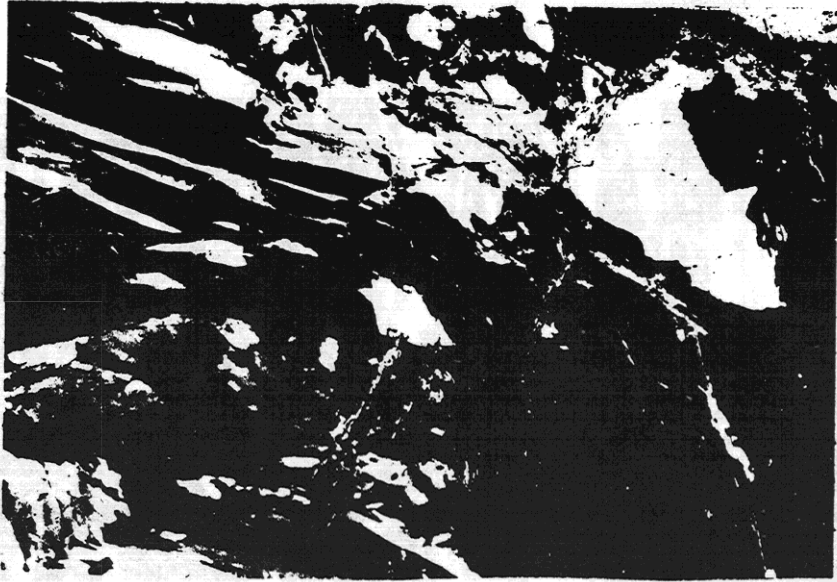
e



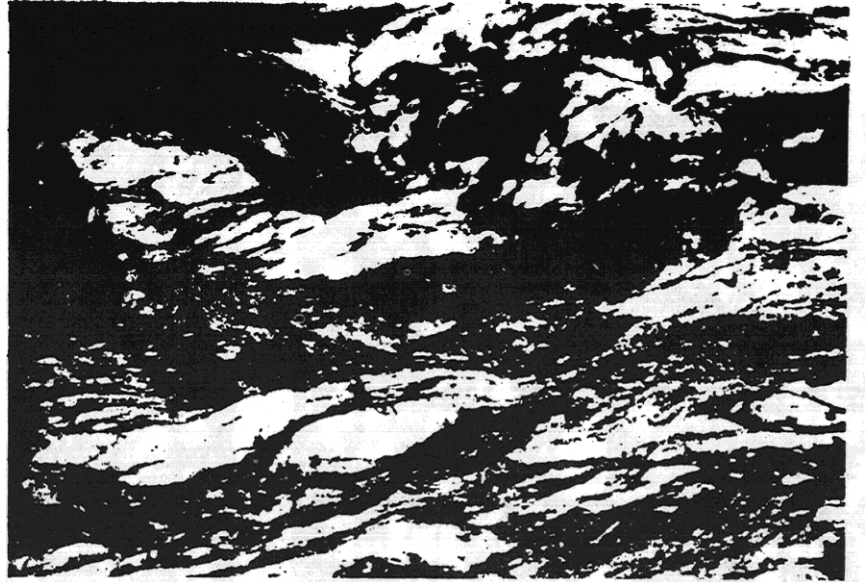
f



49 FIGURE 9



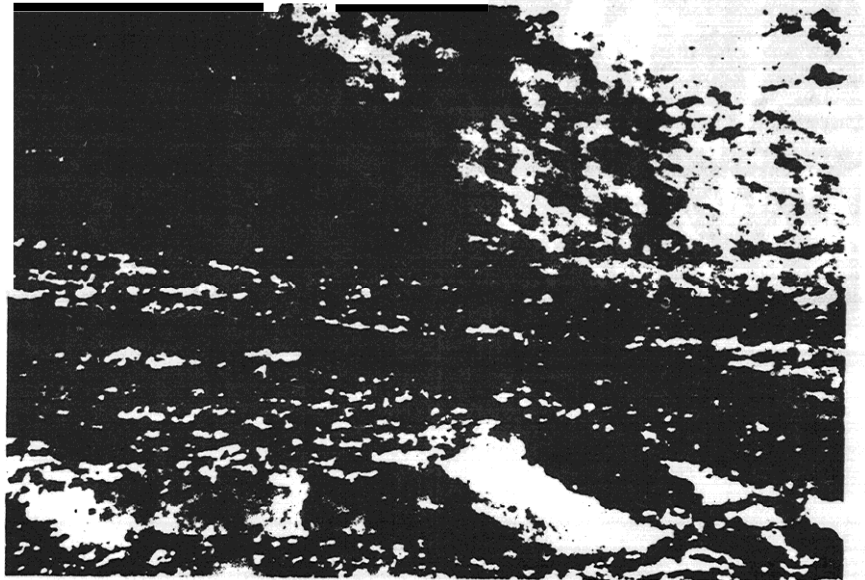
a



b



c



d

FIGURE 10

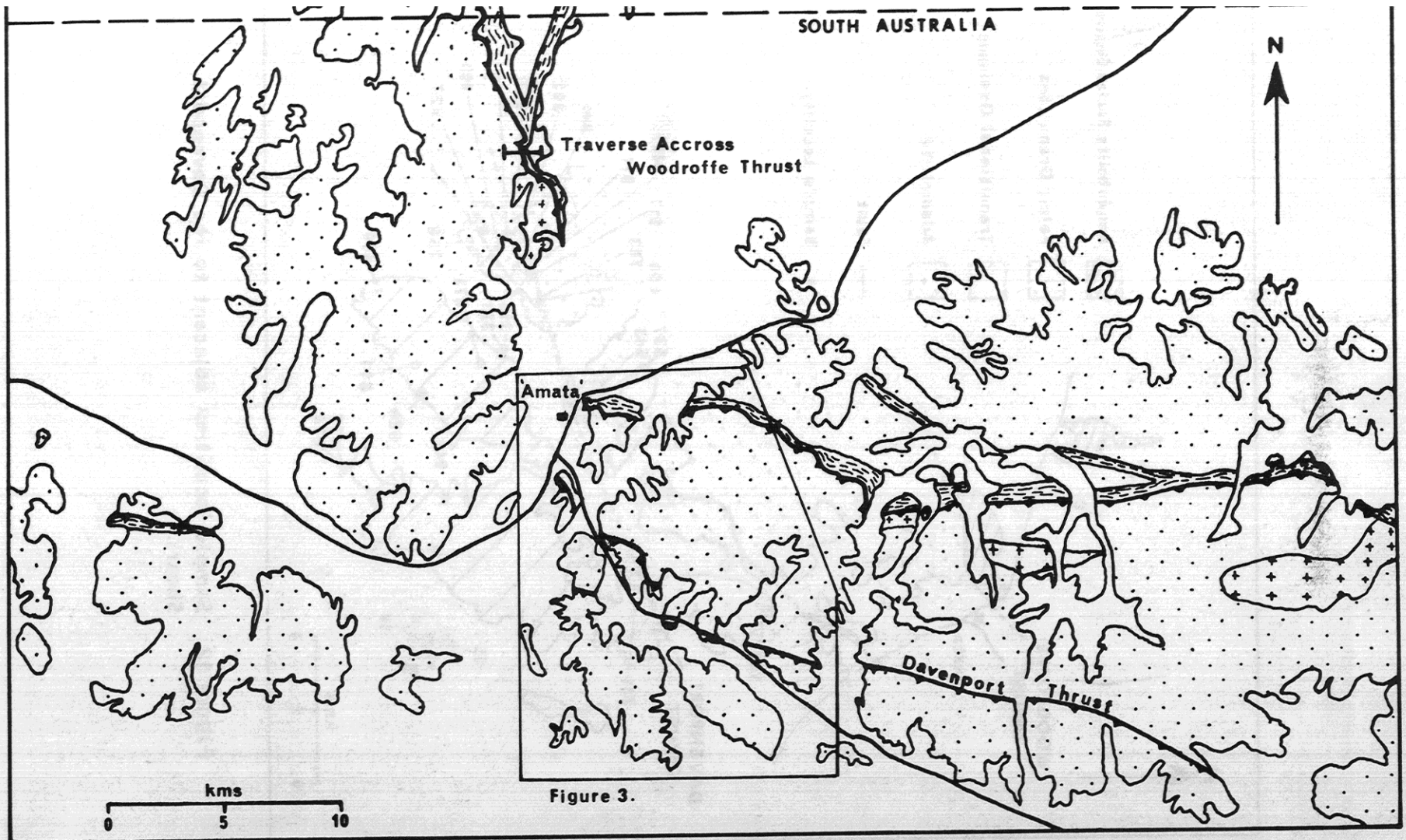


FIGURE 11. GEOLOGICAL MAP OF THE MUSGRAVE RANGES.

— Geological Boundary
 ▼ Thrust
 — Road

□ Quaternary Sediments
 ■ Musgrave - Mann Metamorphic Complex
 ▨ Mylonites and Shear Zones
 ▩ Mafic Intrusives

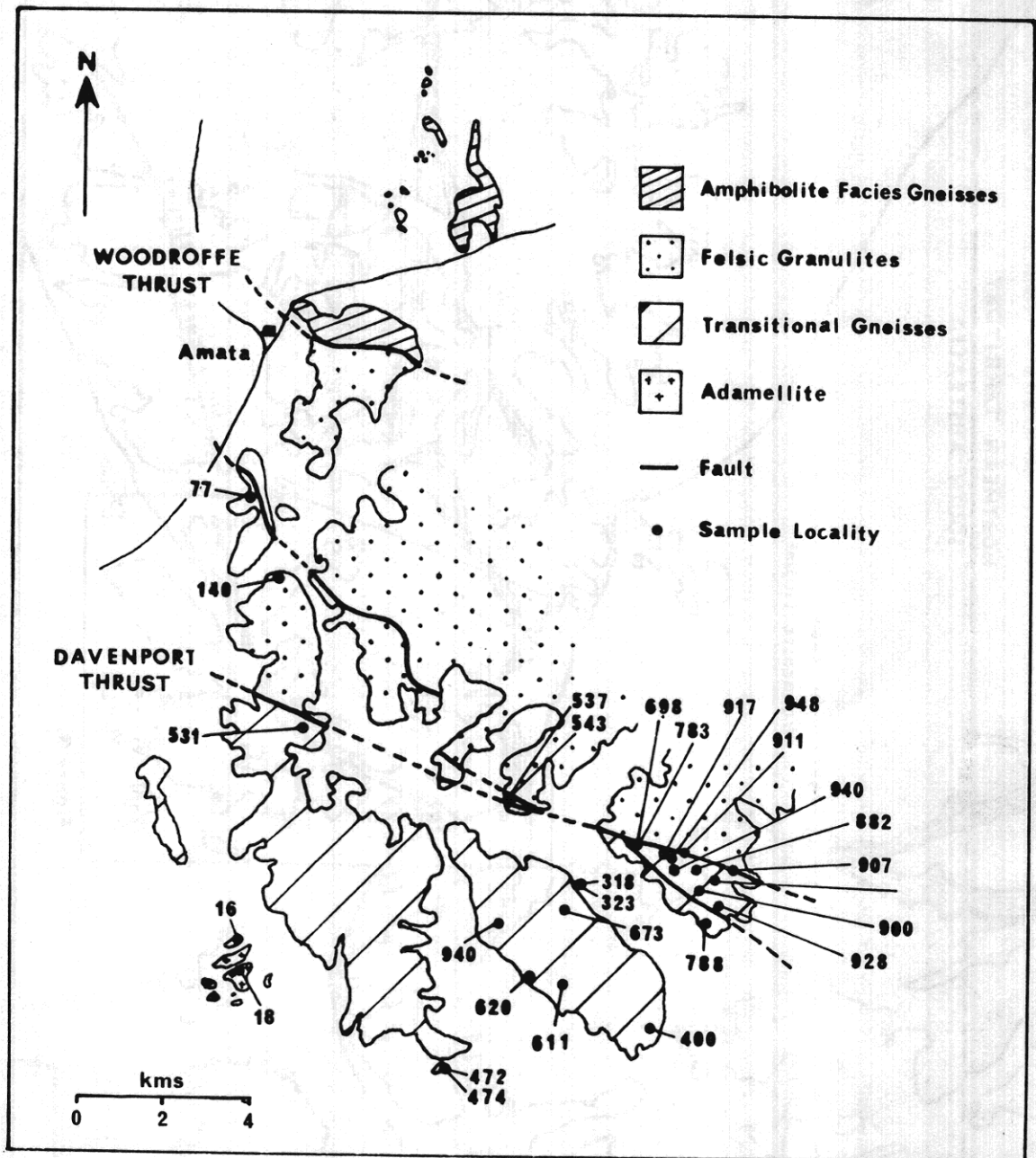


Figure 12. Sample localities adjacent to the Davenport Shear.

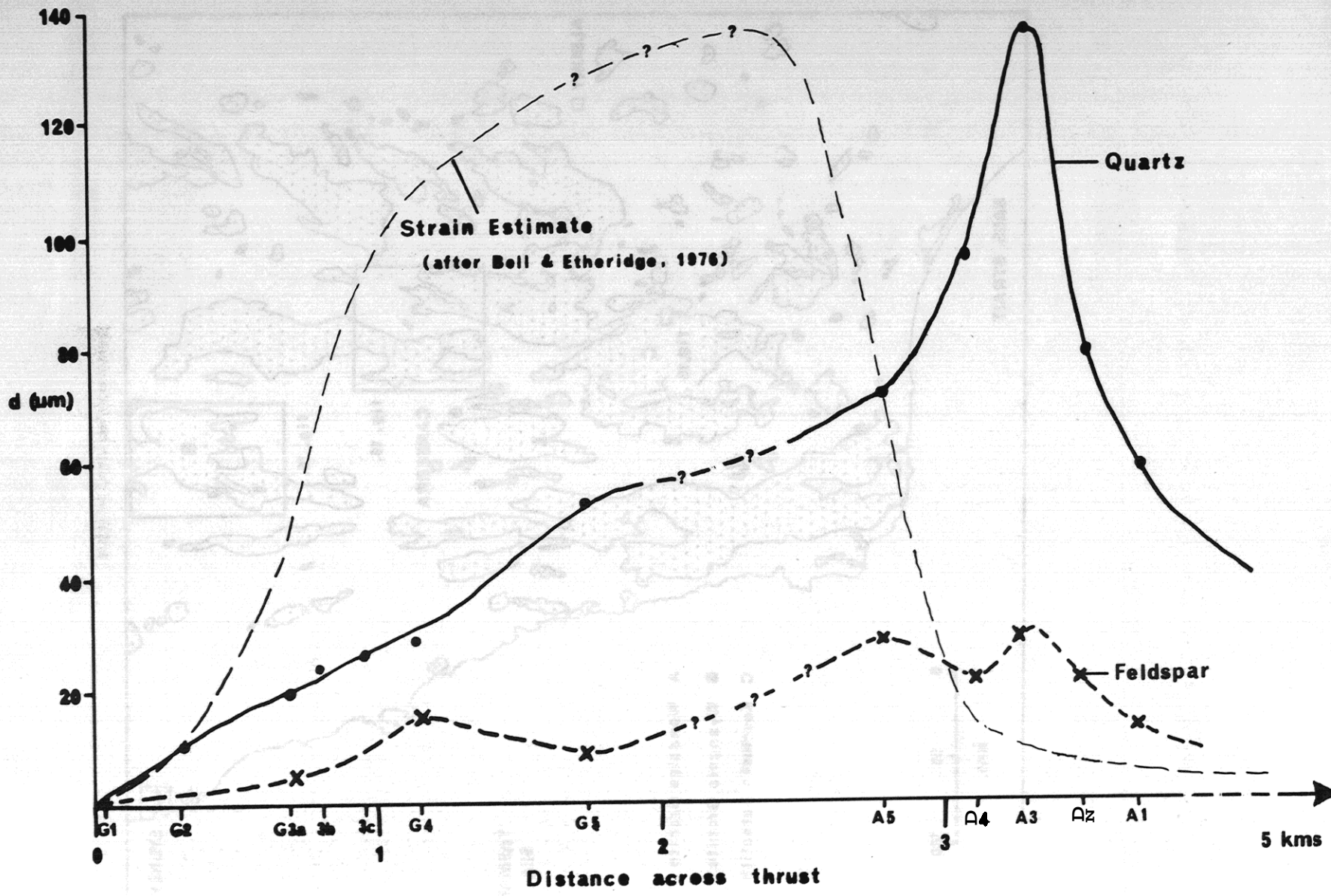
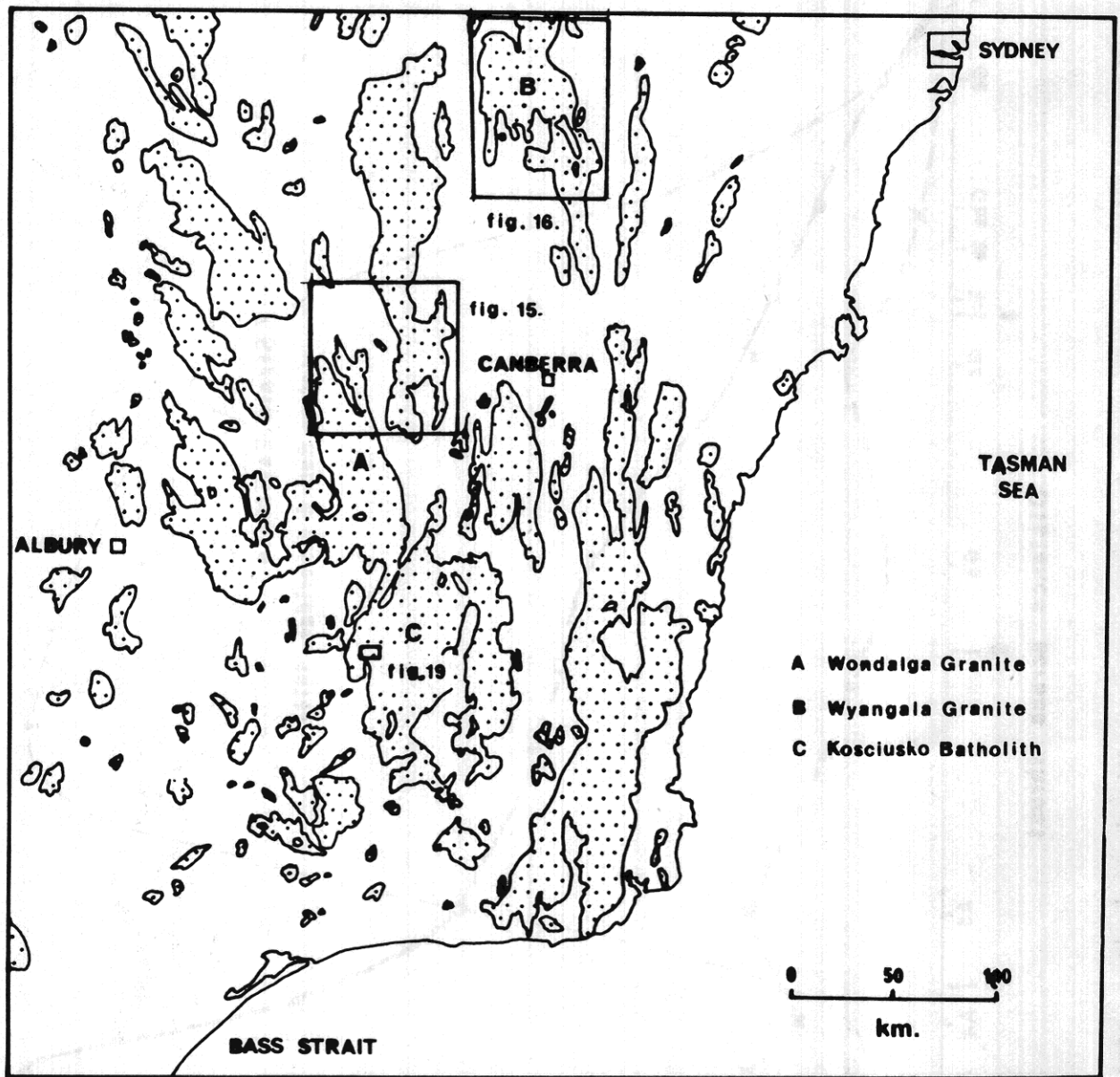


FIGURE 13. Quartz and feldspar recrystallized grainsizes across the Woodroffe Thrust.



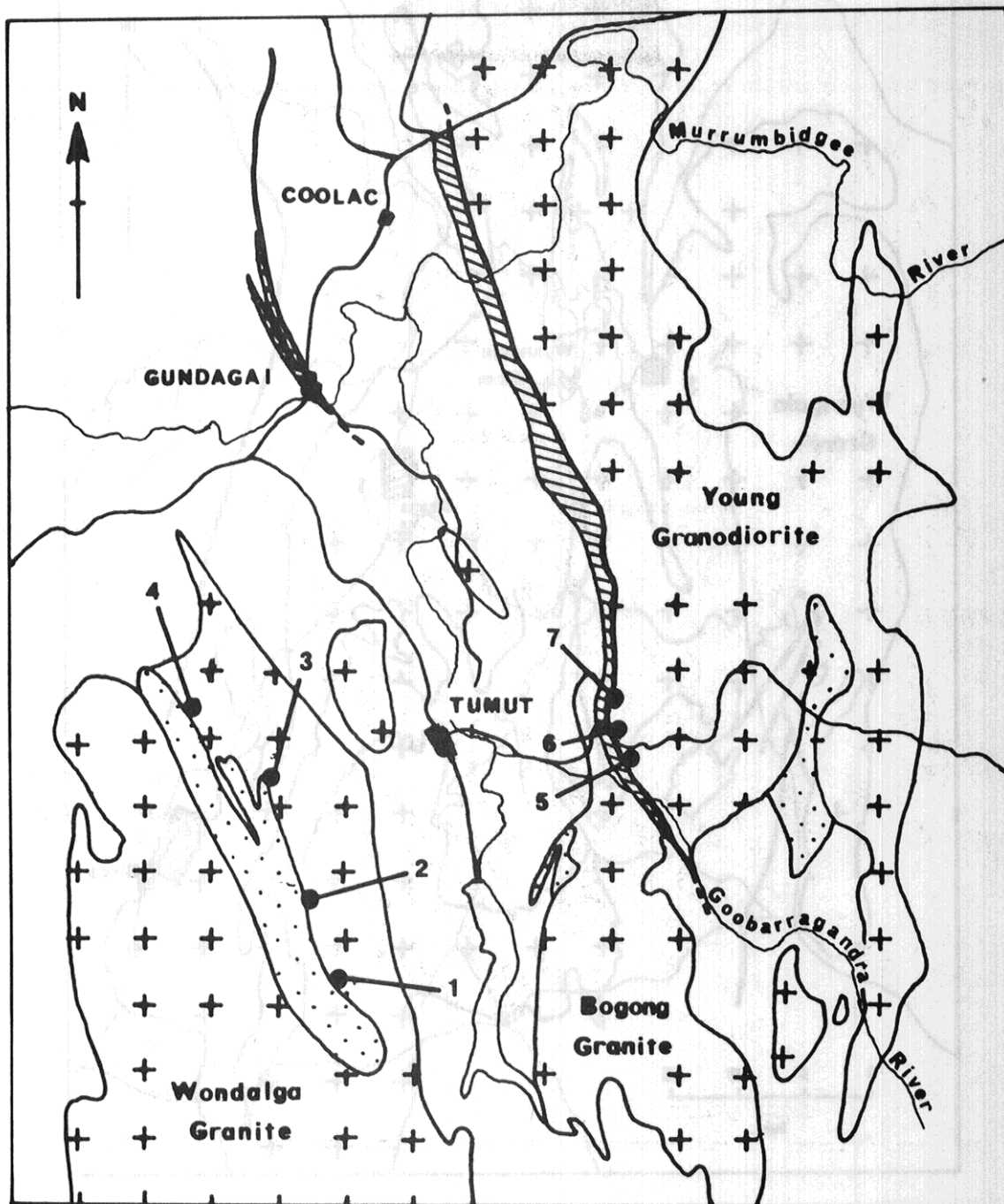


FIGURE 15. Sample locality map for Wondalga Batholith and Coolac Serpentine Belt.

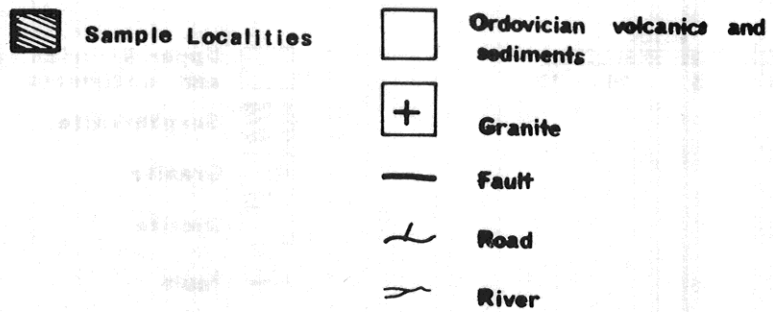
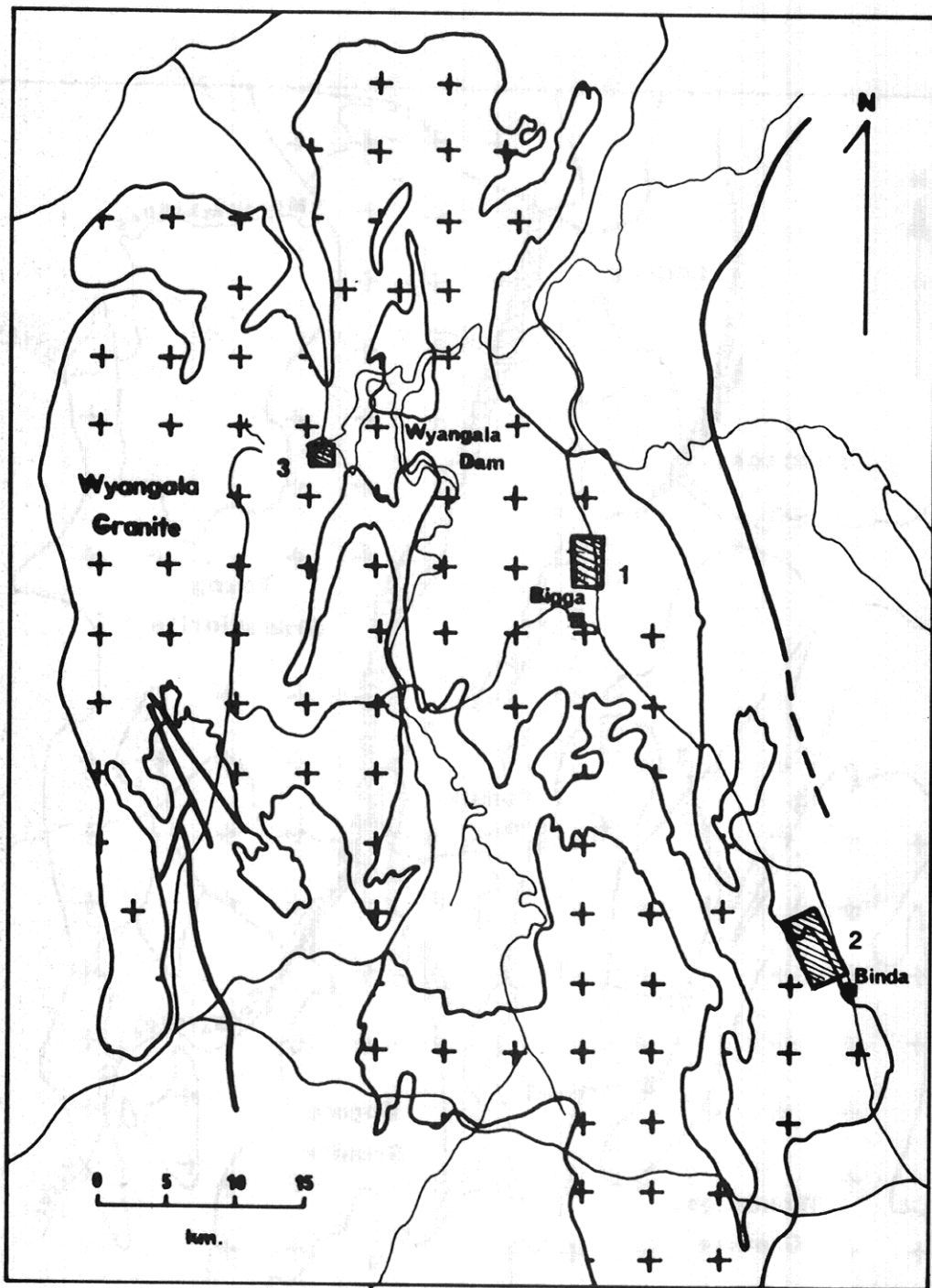
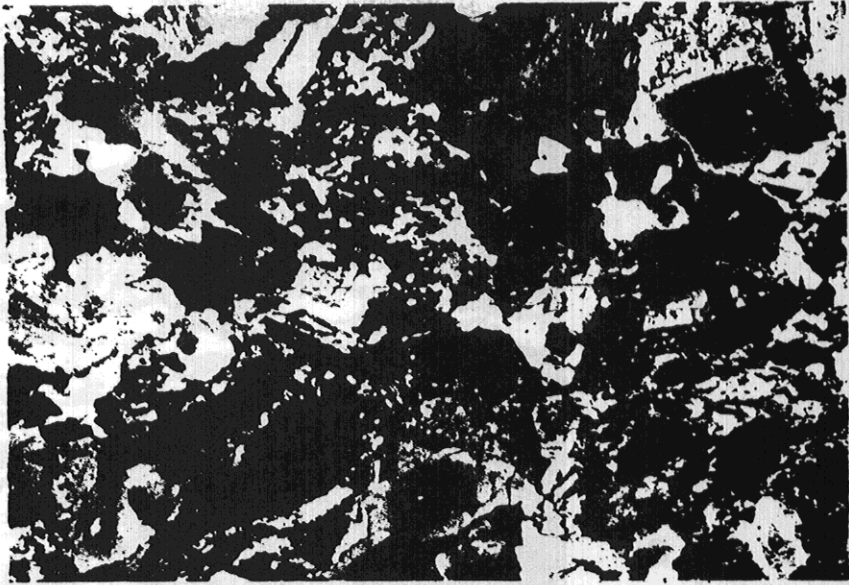
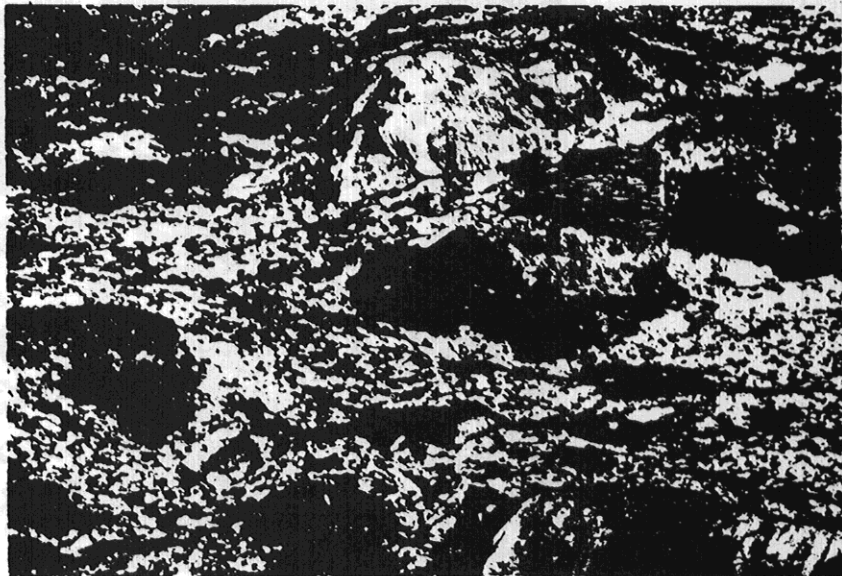


FIGURE 16. Sample localities within the Wyangala Batholith.

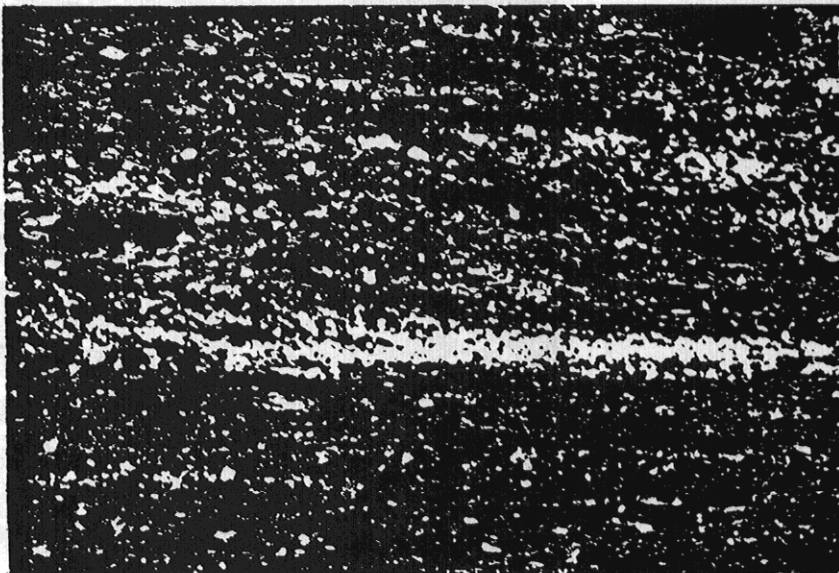
a



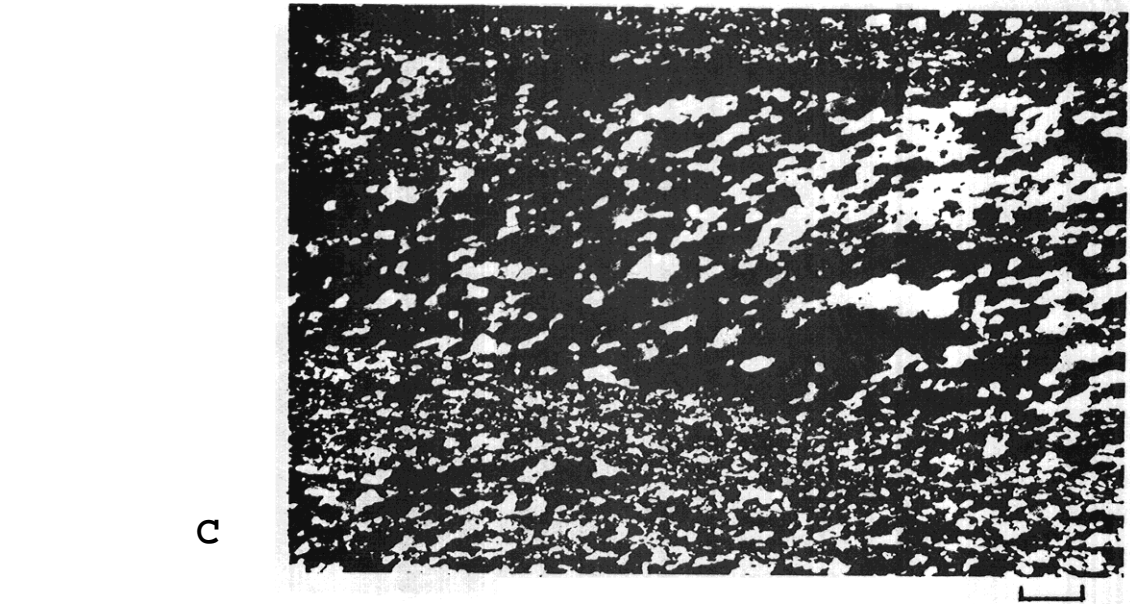
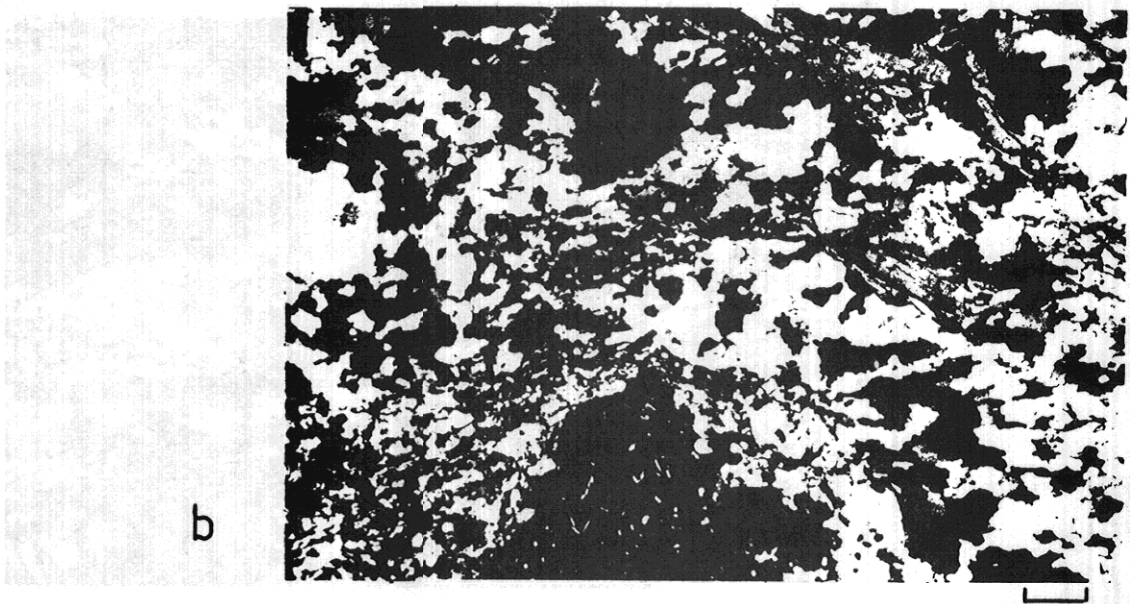
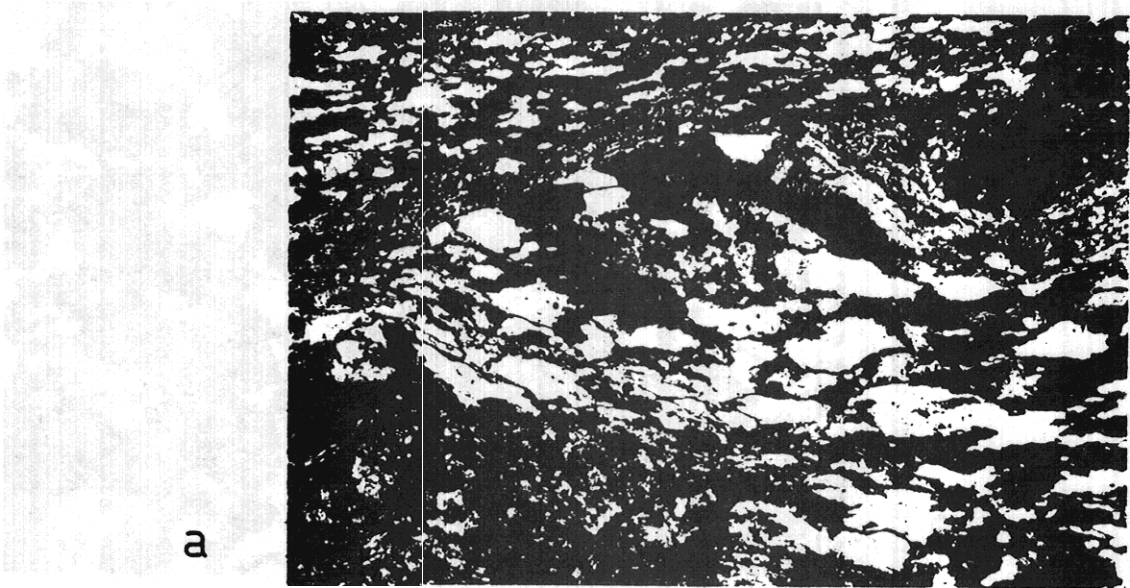
b



c



499 FIGURE 17.



500FIGURE 18

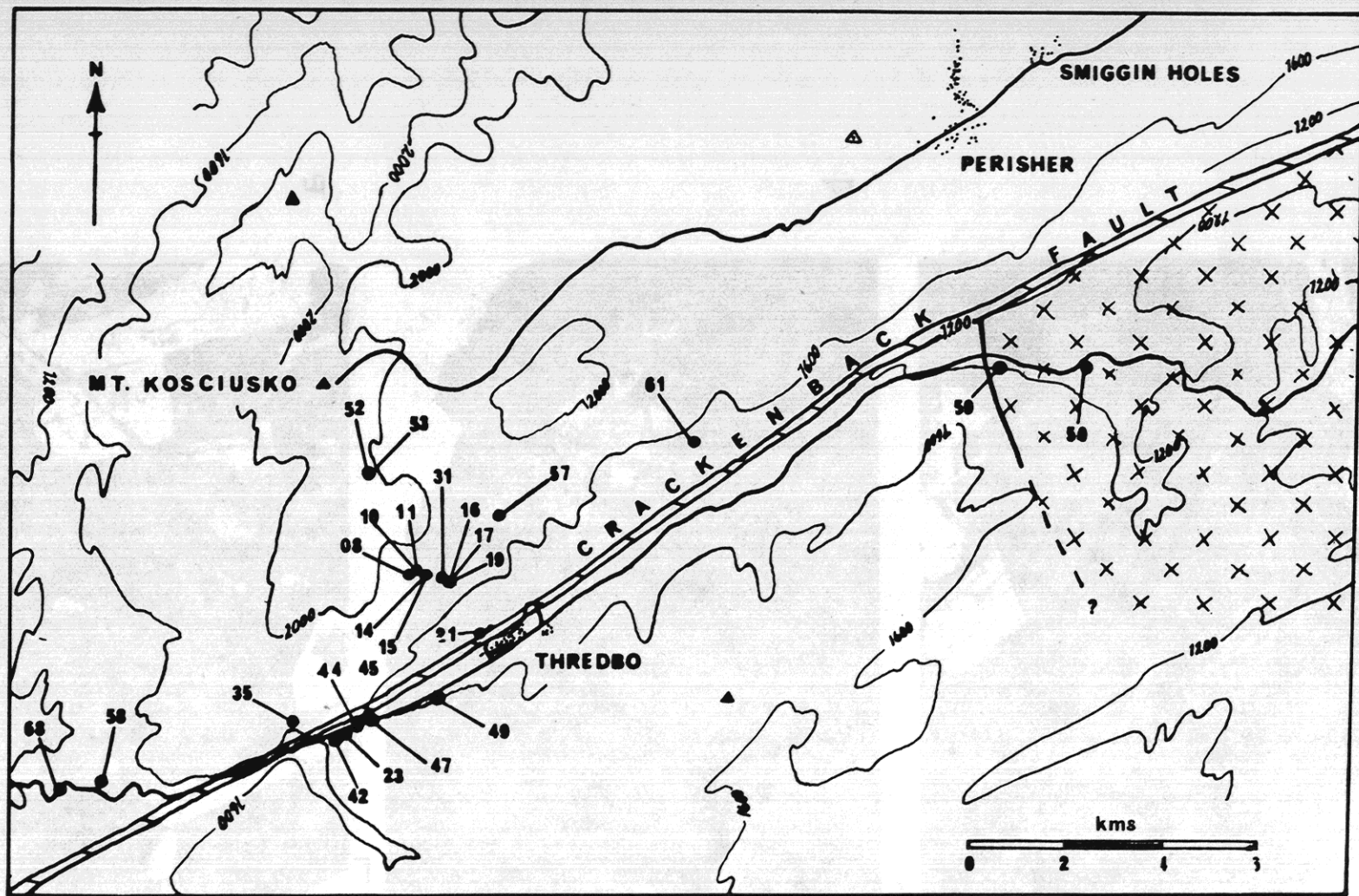
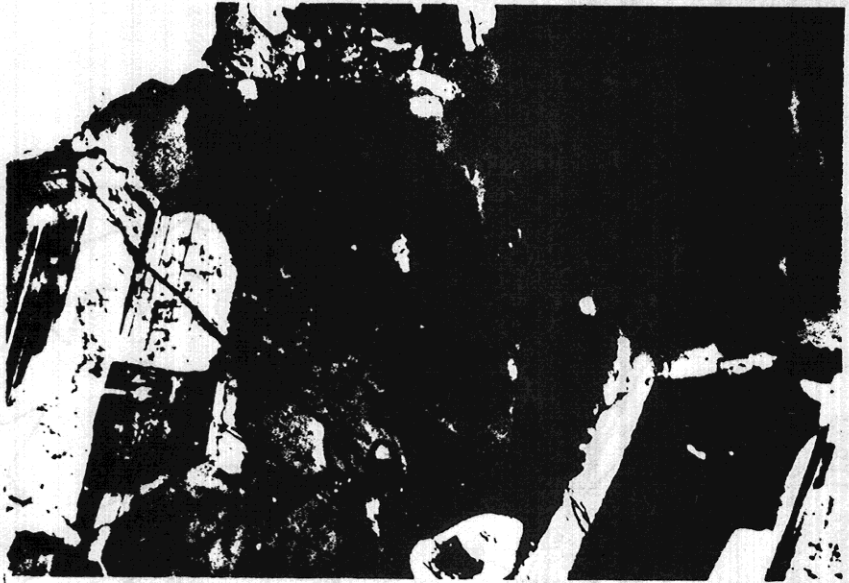


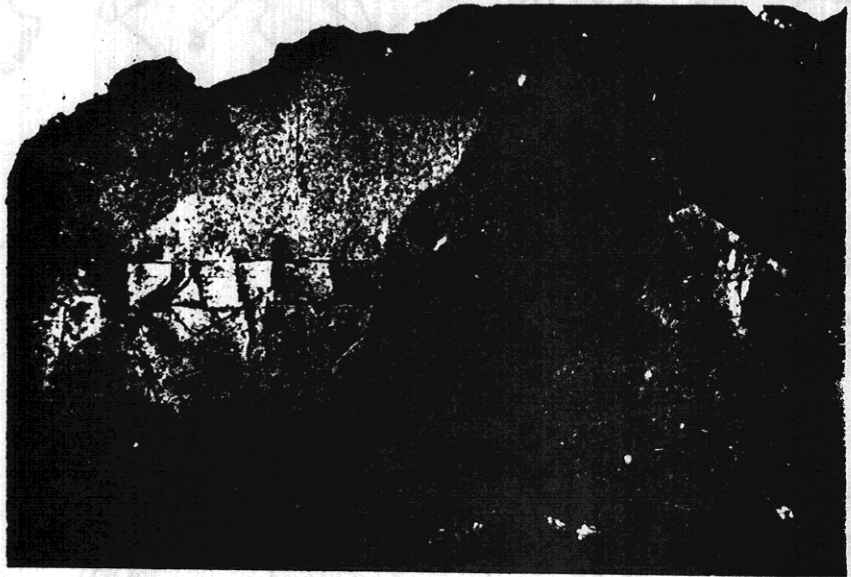
FIGURE 19. Sample localities along the Crackenback fault zone, Mt. Kosciusko area (all sample numbers are pre-1951).

- Wewambah Gneiss (foliated)
- x Massive Granite
- Fault Zone

a



b



c

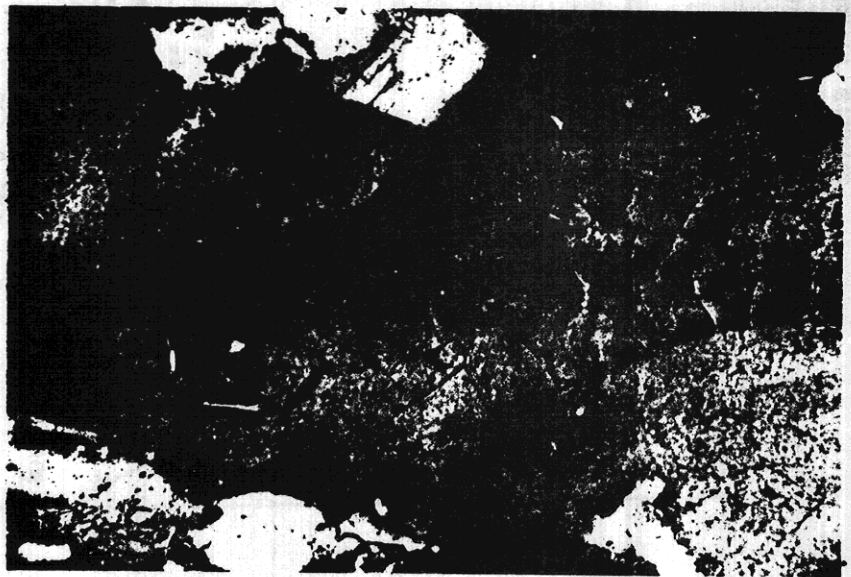


FIGURE 20

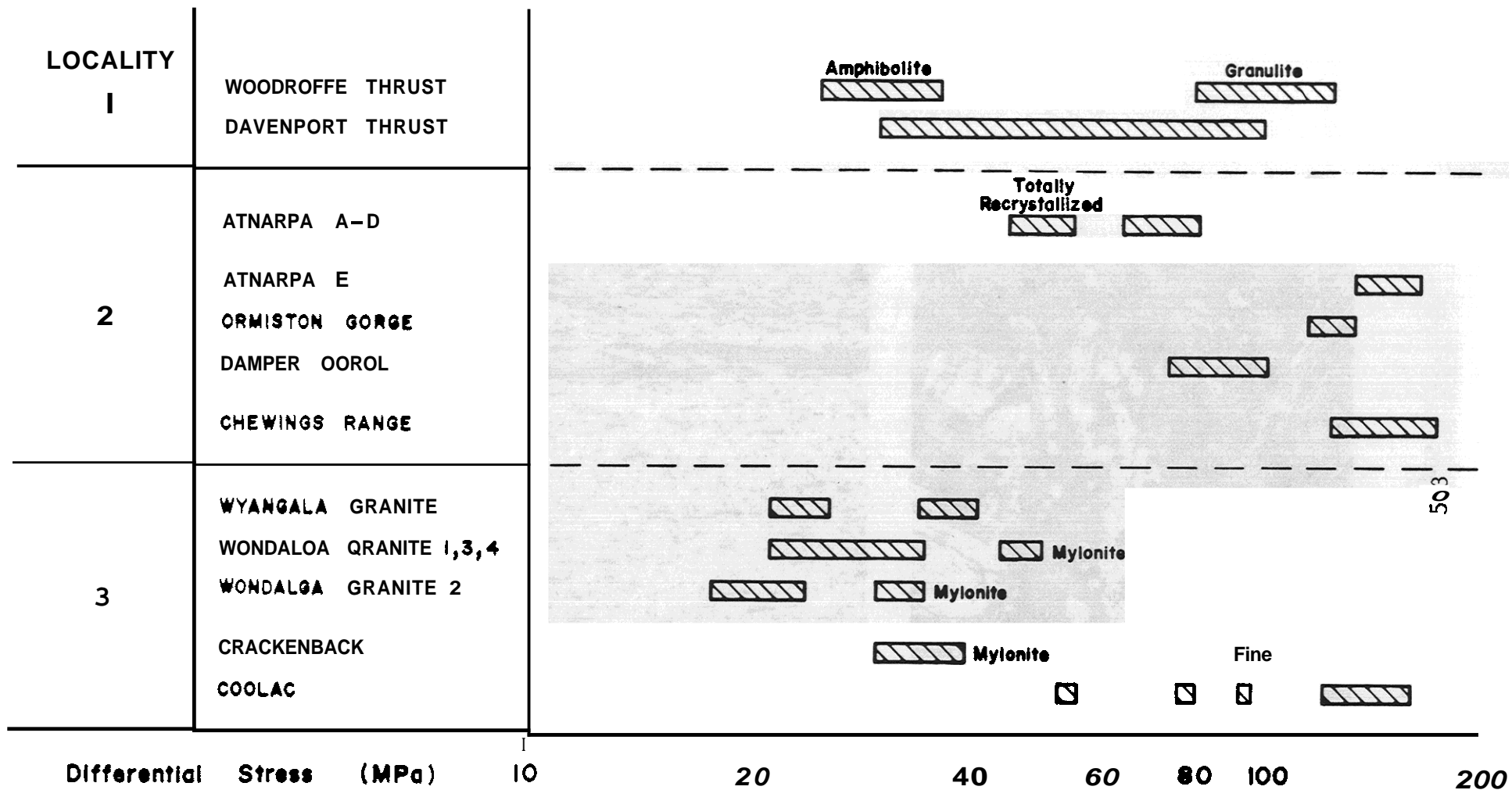
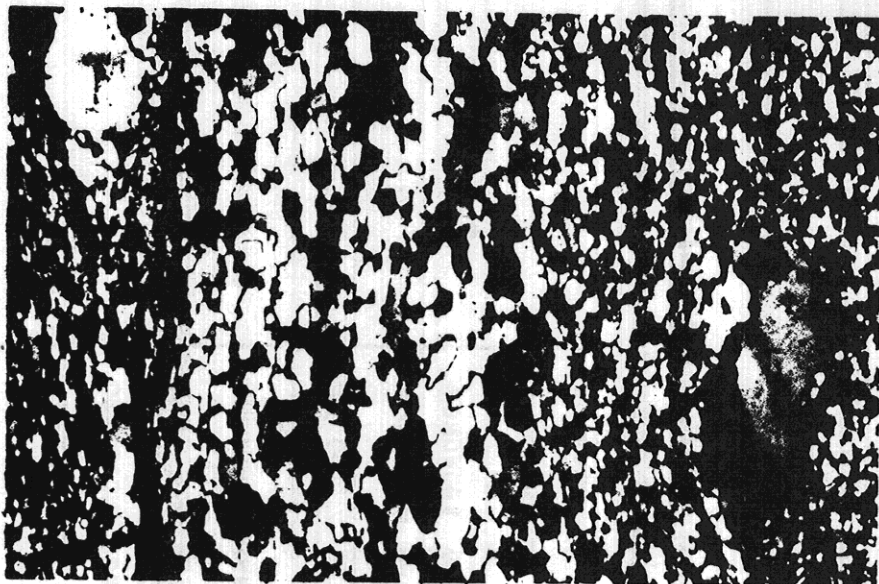


FIGURE 21. Graph summarizing stress values calculated from recrystallized grainsize data.

a



b



c



504 FIGURE 22.